THE PENNSYLVANIA STATE UNIVERSITY
SCHREYER HONORS COLLEGE

DEPARTMENT OF BIOENGINEERING

IMPROVING CARBON FIBER MICROELECTRODE PERFORMANCE FOR MEASURING SEROTONIN BY VOLTAMMETRY

LAUREN ELIZABETH SAWARYNSKI

Spring 2010

A thesis
submitted in partial fulfillment
of the requirements
for a baccalaureate degree
in Bioengineering
with honors in Bioengineering

Reviewed and approved* by the following:

Anne Milasincic-Andrews
Associate Professor of Molecular Toxicology
Thesis Supervisor

William O. Hancock
Associate Professor of Bioengineering
Honors Adviser

Peter J. Butler
Associate Professor of Bioengineering
Faculty Reader

* Signatures are on file in the Schreyer Honors College.

Abstract

The serotonin neurotransmitter system is known to modulate many physiological and psychological functions, including the regulation of sleep, mood, anxiety, and cognition. The overarching goals of the Andrews' research group are to investigate and to understand how the serotonergic system affects brain chemistry and how imbalances in the serotonin system may contribute to the etiology and treatment of psychiatric disorders, particularly anxiety and depression. *In vivo* and *ex vivo* measurements of neurotransmitters, including serotonin, are performed using electrochemical techniques such as voltammetry. For the present research, serotonin release and reuptake were monitored in the mouse brain in real time using carbon fiber microelectrodes in conjunction with voltammetric techniques and a custom built instrument and analysis software. Here, we sought to develop methods for enhancing the performance of carbon fiber microelectrodes to obtain *in vivo* and *ex vivo* serotonin measurements. These improved techniques to detect small but significant changes in the serotonin system will be valuable in advancing our understanding of how serotonin neurotransmission is altered in mood and anxiety disorders.

Acknowledgements

The completion of this thesis and the projects described within would not have been possible without contributions from multiple individuals. First, I owe my deepest gratitude to Prof. Anne Milasincic Andrews for allowing me to be a member of her laboratory for almost three years. The experience and knowledge I have gained while working with Prof. Andrews is invaluable and has helped me to achieve success in many aspects of my academic life. In addition, I would like to thank Yogesh Singh for being an incredibly knowledgeable, encouraging, and supportive mentor during my time spent working in the Andrews' laboratory. I would not have been able to complete the research discussed in this thesis without him. I have also gained a substantial amount of knowledge about many scientific areas due to the diverse experience of the other graduate students I have worked with including Tracy Gilman, Stefanie Altieri, Brendan Beikmann, Amanda Bressler, and Moe Zhao. I would also like to thank my honors advisor, Dr. William Hancock, for his willingness to help me make difficult decisions regarding my academic and future career paths throughout my undergraduate career.

This project was supported by funding from the National Institute of Mental Health (MH064756 to AMA). The content is solely the responsibility of the authors and does not necessarily represent the official views of the National Institute of Mental Health or the National Institutes of Health.

Table of Contents

List of Figures

List of Tables

Chapter 1: Introduction

The human brain is an extremely complicated structure, consisting of approximately 100 billion interacting neurons (E. R. Kandel et al., 2000; L. R. Squire et al., 2008). These neurons communicate with one another via chemical signals to control most bodily functions, to facilitate thought, speech, emotion, and mood, and to allow individuals to interact with their surroundings (E. R. Kandel et al., 2000; J. Nolte, 2002; L. R. Squire et al., 2008). Due to the complexity of the brain and the thousands of chemical signals exchanged by neurons every minute, the brain is simultaneously the least understood and arguably the most important organ in the body.

Among mental disorders, major depressive disorder is a leading cause of disability in the U.S. between the ages of 15-44 (R. C. Kessler et al., 2005b). Additionally, depression has high co-morbidity with anxiety disorders and substance abuse. Anxiety and depressive disorders and their treatment are related to changes in brain chemistry involving the neurotransmitter serotonin (D. L. Murphy et al., 1978; F. G. Graeff, 1997; B. H. Harvey, 1997; D. L. Murphy et al., 1998; E. J. Nestler et al., 2002; C. A. Lowry et al., 2008). The methods most commonly used *in vivo* to investigate changes in serotonin neurochemistry in animal studies include microdialysis and carbon fiber voltammetry. Chronoamperometry and fast cyclic voltammetry are two electroanalytical voltammetry techniques that are explored in detail throughout this thesis. Carbon fiber voltammetric methods, although widely used to study *in vivo* dopamine neurotransmission, are not frequently used to study *in vivo* serotonin neurotransmission due to many challenges. Unlike dopamine, serotonin neurotransmission occurs in most brain regions and it is

hypothesized that the amount of serotonin released during neuronal excitation is very low. Additionally, long term *in vivo* serotonin measurements using carbon fiber microelectrodes lead to electrode fouling due to exposure to biological tissue and to serotonin itself, thus affecting reliable estimations of serotonin concentrations. The work carried out for this thesis has attempted to approach and to solve some of these problems by optimizing a number of aspects of carbon fiber voltammetry specifically to sense serotonin *in vivo* and *in vitro*. Herein, we seek to study and to understand how serotonin affects bodily responses, particularly with regard to the etiology of anxiety and depression disorders. We aim to monitor serotonergic neurotransmission in the mouse brain with high temporal resolution to measure serotonin release and reuptake in real time.

1.1 The serotonergic system and mood disorders

The National Institutes of Health estimates that 20 million Americans currently suffer from clinical depression, a condition that negatively affects many, if not all, aspects of life (NIH, 2010). Symptoms of depression include overwhelming sadness, changes in sleep patterns, loss of interest in previously enjoyable activities, and even thoughts of or attempts at suicide (NIH, 2010). Anxiety disorders are also prevalent in the United States, as an estimated 40 million adults suffer from some form of an anxiety disorder (which includes generalized anxiety disorder, panic disorder, obsessive compulsive disorder, various phobias, and post traumatic stress disorders) (R. C. Kessler et al., 2005a; E. D. Leonardo and R. Hen, 2008; NIMH, 2009). Enumerable studies have implicated serotonin as a major player in the development of many types of mood

disorders including anxiety and depression (S. C. Risch and C. B. Nemeroff, 1992; M. J. Owens and C. B. Nemeroff, 1994; F. G. Graeff, 1997; D. L. Murphy et al., 1998; E. J. Nestler et al., 2002; C. A. Lowry et al., 2008).

The serotonin neurotransmitter system is regulated by 15 different receptors and a transporter (SERT). The serotonin receptors located on both pre- and postsynaptic neurons are responsible for sensing serotonin that has been released into the extracellular space by presynaptic neurons (F. G. Graeff, 1997; M. Filip and M. Bader, 2009). Stimulation of serotonin receptors begins a cascade of events, which allows the signal sent by presynaptic neurons to have effects on membrane polarization, intracellular signaling, and gene expression. Fifteen molecularly unique serotonin receptors have been characterized in vertebrates (D. L. Murphy et al., 1998; M. Filip and M. Bader, 2009). This wide array of different serotonin receptors is attributed to evolutionary adaptations that have allowed serotonin to develop effects on multiple bodily systems and functions (D. L. Murphy et al., 1998). While many different serotonin receptors exist, only one serotonin transporter has been identified. The function of the serotonin transporter is to clear released serotonin from the extracellular space thus terminating the stimulation of the serotonin receptors (M. J. Owens and C. B. Nemeroff, 1994; D. L. Murphy et al., 1998; D. L. Murphy et al., 2001).

The serotonin transporter has been frequently targeted pharmacologically in the treatment of depressive disorders or other problems related to serotonin imbalances of the brain by drugs called selective serotonin reuptake inhibitors (SSRIs) (R. W. Fuller, 1994; D. J. Nutt et al., 1999; D. L. Murphy et al., 2004). The positive effects of SSRIs on

depression were initially discovered accidentally when their application was found to alleviate symptoms of depression (D. L. Murphy et al., 1986). This led to the development of the monoamine hypothesis of depression. According to this hypothesis, many antidepressants function by blocking the reuptake of serotonin by serotonin transporters, thus increasing extracellular serotonin concentrations and increasing serotonin receptor activation (R. W. Fuller, 1994; A. Frazer, 1997; B. H. Harvey, 1997; E. J. Nestler, 1998; T. A. Mathews et al., 2000). However, acute administration of SERT inhibitors is not sufficient; rather, a number of weeks of chronic administration is needed for these drug to show efficacy (B. H. Harvey, 1997; M. A. Katzman, 2009). Furthermore, increases in extracellular serotonin level after chronic antidepressant treatment is not well established (A. M. Andrews, 2009). Investigations into the molecular mechanisms of the effects of SSRIs on SERT revealed that the drugs block the transporter in a matter of hours (D. L. Murphy et al., 1998; D. J. Nutt et al., 1999; D. L. Murphy et al., 2004). The reasons behind the delayed efficacy of SSRIs are not fully understood, but data from many studies indicate that the antidepressant effects of SSRIs are not solely due to increases in extracellular serotonin but also to long-term pre- and post-synaptic adaptive responses that occur in response to consistent increases in extracellular serotonin (D. L. Murphy et al., 2004).

Further studies using selective serotonin reuptake inhibitors such as citalopram, fluoxetine, and paroxetine have been performed to study their effects on the serotonin system (R. Invernizzi et al., 1992; K. W. Perry and R. W. Fuller, 1992; G. Pineyro and P. Blier, 1999). Results from these studies showed that high doses of SSRIs result in

significantly higher concentrations of extracellular serotonin in acute time periods (Y. Chaput et al., 1986; G. Pineyro and P. Blier, 1999). However, the doses of the SSRIs used were 15-35 times greater than the therapeutic dose (G. Pineyro and P. Blier, 1999). Chronic treatments with lower doses of SSRIs failed to show acute increases in extracellular serotonin concentrations, but after two weeks, increases in extracellular serotonin concentrations were seen that were similar to the levels produced by the acute, high dose models (Y. Chaput et al., 1986; R. Invernizzi et al., 1994; G. Pineyro and P. Blier, 1999). The mechanisms underlying the differences between acute and chronic effects are not yet fully understood (G. Pineyro and P. Blier, 1999).

In addition to pharmacologic methods of targeting the serotonin neurotransmitter system, mice have been genetically engineered by modifying the gene that codes for the serotonin transporter (SERT) (K. P. Lesch et al., 1996). It was determined that this gene in humans contains a promoter region polymorphism that alters the expression of the SERT gene (A. Heils et al., 1997; B. D. Greenberg et al., 1999; D. L. Murphy et al., 2001). Genetically engineered mice, called knockout mice, (either heterozygous +/-, or homozygous -/-) are used to study the effects of constitutive loss of SERT on serotonergic neurotransmission. Mice with genetic reductions in SERT expression showed strain dependent increases in anxiety-like phenotypes (A. Holmes and A. R. Hariri, 2003), among many other serotonin-related changes in phenotype (D. L. Murphy et al., 2008). *In vivo* microdialysis studies in SERT knockout mice revealed that complete loss of serotonin transporter expression in SERT -/- mice resulted in a large 5-fold increase in extracellular serotonin (T. A. Mathews et al., 2004). SERT knock-out

mice show increases in anxiety, stress, and fearfulness as compared to SERT +/+ mice, as determined by a variety of behavioral tests (Q. Li et al., 1999; D. L. Murphy et al., 2001; A. Holmes et al., 2002; A. Holmes and A. R. Hariri, 2003; A. Holmes et al., 2003). These findings complicate the theory that increased extracellular serotonin levels improve symptoms of anxiety and depressive disorders, and indicate that there is more underlying the function of SSRIs and SERT than was initially imagined.

In addition to the results from studies in SERT knockout mice, investigations have been performed on the serotonin transporter-linked polymorphic region (5-HTTLPR) of the SERT gene in humans. Studies by Lesch *et al.* have shown that the short "s" allele of this promoter region polymorphism is linked to lower transcriptional efficiency, and lower SERT expression as compared to the long "l" allele, which lacks a specific 43-base pair region (K. P. Lesch et al., 1996). Further studies in humans showed that individuals harboring an s allele (either heterozygous, s/l, or homozygous, s/s) exhibit increased neuroticism and increased likelihood to develop anxiety or depression after a stressful life event as compared to individuals that are homozygous for the long allele of the 5-HTTLPR (K. P. Lesch et al., 1996; A. Caspi et al., 2003). Two meta-analysis studies on the effects of the h5-HTTLPR on anxiety-related personality traits showed evidence for an association between the short form of the 5-HTTLPR allele and neuroticism, but not with other anxiety-like personality traits (J. A. Schinka et al., 2004; S. Sen et al., 2004). This variance in the results can be attributed to the presence of other polymorphisms in the human SERT gene. Research on the effects of the 5-HTTLPR on serotonin neurotransmission have also produced mixed results with some studies showing a

decrease in SERT expression, and/or serotonin uptake (B. D. Greenberg et al., 1999; G. M. Anderson et al., 2002; Y. Singh et al., 2009) associated with the "s" allele, while others show no changes in SERT expression and/or serotonin uptake (A. A. Patkar et al., 2004; R. V. Parsey et al., 2006). However, pharmacologic inhibition of SERT in postnatal mice produces an altered phenotype during adulthood characterized by increased depressive-like behavior (M. S. Ansorge et al., 2004; M. S. Ansorge et al., 2008; D. Popa et al., 2008). These studies suggest that SERT inhibition during key developmental periods might be one of the factors responsible for altered behavior observed in SERT-deficient mice or humans with the 5-HTTLPR "s" allele.

To summarize, many different methods and models have been used to understand the effects of changes in the serotonergic neurotransmitter system on behavior and anxiety and depression disorders. This research has resulted in some insight into the role of serotonin in the brain with regard to anxiety and depression disorders and reinforces the role of serotonin system in mood and anxiety disorders. However, the mechanisms of action of SSRIs and the exact development of the phenotypic expression of anxiety and depression due to changes in the serotonergic system are not yet fully understood.

1.2 Electroanalytical methods to measure serotonergic neurotransmission

To monitor neurotransmission in the brain, several different techniques have been used. These involve implanting probes into the brain for neurochemical detection. Microdialysis is a well accepted method of measuring changes in extracellular

neurotransmitter levels, however, it has relatively poor temporal resolution (T. E. Robinson and J. B. Justice, 1991). This means that the lag time between neurotransmission events, in which a particular neurotransmitter of interest is released, and the time at which the microdialysis system recognizes the increase in neurotransmitter concentration is quite long (on the order of minutes), making it difficult to detect rapid changes in neurotransmitter concentration (T. E. Robinson and J. B. Justice, 1991). Therefore, the microdialysis technique is primarily used to monitor basal levels of neurotransmitter *in vivo* (T. E. Robinson and J. B. Justice, 1991).

In order to gain a better understanding of serotonergic neurotransmission, it is also necessary to measure serotonin release and reuptake in the brain in real time with sub-second scale temporal resolution. Thus, voltammetry techniques like fast cyclic voltammetry (with temporal resolution of 100 milliseconds) and chronoamperometry (temporal resolution of a second) are complimentary techniques to microdialysis (temporal resolution in minutes), and are better suited for studying the fast kinetics of neuronal release (R. M. Wightman, 1988; T. E. Robinson and J. B. Justice, 1991; D. J. Michael and R. M. Wightman, 1999). A qualitative comparison of electroanalytical techniques can be found in Figure 1.1.

Voltammetry for neurotransmitter detection makes use of carbon fiber microelectrodes, a potentiostat, and a custom computer program to monitor neurotransmitters either *in vitro* or *in vivo* (K. T. Kawagoe et al., 1993; D. J. Michael and R. M. Wightman, 1999). Monoamine neurotransmitters, or neurotransmitters that contain one amino group attached to an aromatic ring via a two carbon chain, as can be

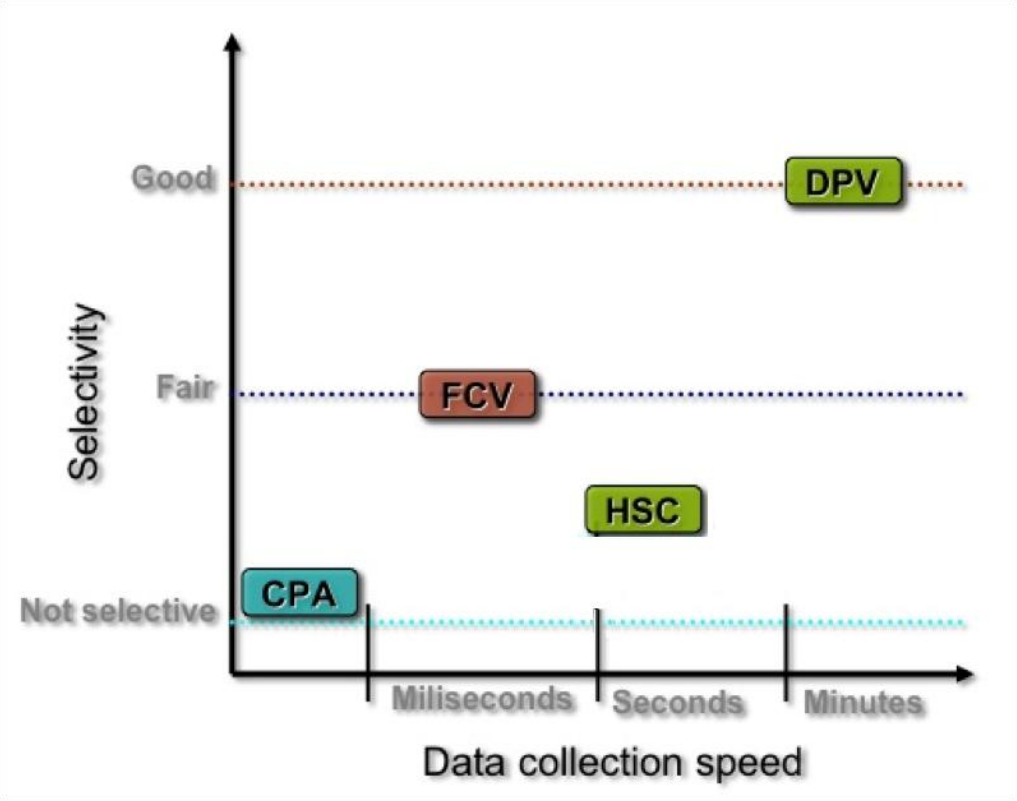

Figure 1.1: Comparison of electroanalytical techniques. This diagram shows the benefits and drawbacks of the multiple types of voltammetry techniques. Constant potential amperometry (CPA), high-speed chronoamperometry (HSC), fast cyclic voltammetry (FCV), and differential pulse voltammetry (DPV) are depicted here. The two techniques that are the focus of this thesis are HSC and FCV.

seen in Figure 1.2, and many other neurochemicals are electroactive in nature. Electroactive neurotransmitters are those that can be oxidized and/or reduced via the application of a sufficient voltage (typically less than 1 V), and thus can be detected using electrochemical methods like carbon fiber voltammetry. Due to the small size, straight forward fabrication, low background current, and reduced IR drop of carbon fiber microelectrodes (CFMs), these probes are well suited for neurotransmitter measurements in the mouse brain *in vivo*. Application of a potential to CFMs that is higher than the oxidation potential of the neurotransmitter species of interest leads to oxidation of that neurotransmitter liberating electrons. Upon the oxidation of serotonin, two electrons are generated. These electrons are subsequently sensed by CFMs. According to Faraday's law, the change in the current detected by a sensor is directly proportional to concentration of the species in solution that is oxidized or reduced. During the reduction step, oxidized serotonin is reduced and the electrode measures a change in current that is proportional to the amount of oxidized serotonin species that has been reduced.

In voltammetry experiments, the responses of individual electrodes to serotonin are calibrated for known concentrations of serotonin or other neurotransmitters of interest. These calibration curves are then used to calculate the amount of serotonin oxidized or reduced during *ex vivo* or *in vivo* experiments.

The most common types of electroanalytical techniques that are used for monitoring neurotransmitters *in vivo* and *in vitro* are constant potential amperometry (CPA), high-speed chronoamperometry (HSC), fast cyclic voltammetry (FCV), and

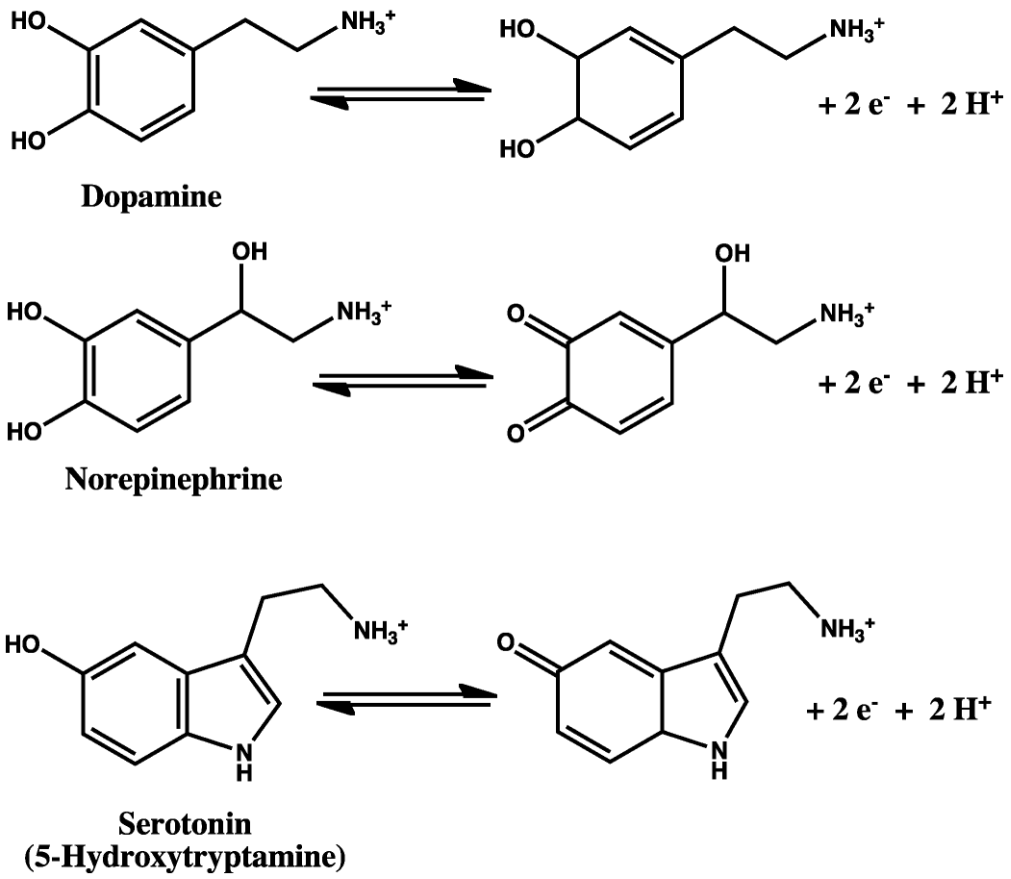

$$Q = n F e$$

Q is the total charge generated (coulombs)
n is the number of moles of a species undergoing oxidation or reduction
F is Faraday's constant (96,487 C/mol)
e is the number of electrons per molecule lost or gained

Figure 1.2: Monoamine redox reactions. When a voltage is applied to carbon fiber microelectrodes placed either in solution or in the mouse brain, neurotransmitter molecules such as dopamine, norepinephrine, or serotonin that are close to the electrode surface are oxidized, releasing electrons near the electrode surface.

differential pulse voltammetry (DPV). Chronoamperometry and fast cyclic voltammetry are the focus of this thesis.

1.2.1 Chronoamperometry

Chronoamperometry is a type of step potential voltammetry. As the name suggests, a time-resolved square wave step potential is applied at the surface of an electrode and the resulting current changes are measured as a function of time. The usual waveform of a chronoamperometric experiment to detect serotonin consists of two steps of 100 ms duration followed by 800 ms of resting time. The first step is the oxidation step, where the potential is increased to a value above the oxidation value of the species of interest, while in second step (the reduction step) the potential is stepped down to a resting value. In the oxidation step, serotonin near the surface of the electrode is oxidized and a faradaic current due to the oxidation is measured at the surface of the electrode by the instrument. Similarly, in the reduction step, oxidized serotonin species will be reduced back to serotonin, generating another faradaic current response at the electrode and instrument (R. M. Wightman, 1988; K. T. Kawagoe et al., 1993). Due to the sharp increase in potential, the initial current measured at the surface of an electrode is predominantly a charging current. Within a short amount of time, the charging current decays at an exponential rate, and the current observed at the electrode surface is predominantly faradaic current. Current values are measured for the duration of the oxidation and reduction steps, but only last 80% of the current value at each step is integrated to give a faradaic current response. Calibration curves are

then constructed by measuring the faradaic current responses of an electrode to various concentrations of a given species. This calibration curve is used to measured changes in the concentration of neurotransmitters in *in vivo* or *ex vivo* experiments using that electrode. Typical excitation and response waveforms from a chronoamperometry experiment are shown in Figure 1.3.

The main advantage of using chronoamperometry over other techniques, including fast cyclic voltammetry, is that chronoamperometry has better sensitivity and can detect small amounts of neurotransmitters in solution. Also, signal to noise ratios are better than in fast cyclic voltammetry. In chronoamperometry, the current measured in a step is integrated for the whole duration of the step leading to a high signal to noise ratio compared to fast cyclic voltammetry (K. T. Kawagoe et al., 1993).

One of the main disadvantages of chronoamperometry, as compared to fast cyclic voltammetry, is that since chronoamperometry uses a stepped potential, it is less selective for a particular species in solution (K. T. Kawagoe et al., 1993). Any species with an oxidation potential less than the applied potential will be oxidized and will contribute to total current measured at electrode. However, ratios of integrated oxidative to reductive currents can be used to identify some species in solution (K. T. Kawagoe et al., 1993).

1.2.2 Fast cyclic voltammetry

Fast cyclic voltammetry is a type of sweep potential voltammetry. A potential is applied in a linear sweep at the electrode surface and the resulting current changes are

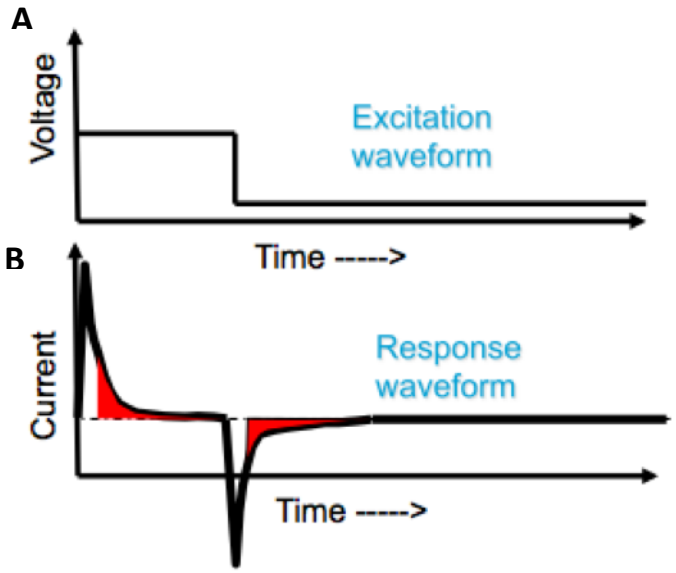

Figure 1.3: Chronoamperometry excitation and response waveforms. Typical chronoamperometry waveform **(A)** consists of an oxidation and reduction step followed by resting period where the potential is held at the reduction potential value. **(B)** Abrupt changes in potential lead to initially high oxidative or reductive non-faradaic charging currents due to Hemholtz layer formation at the electrode surface. Charging currents dissipate exponentially with time. Faradaic current, which is proportional to the species of interest, is integrated for the last 80% of each scan to minimize contributions from charging currents. Integration of this predominantly faradaic current leads to high signal to noise ratios.

measured as a function of time. The usual waveform of a fast cyclic voltammetry experiment consists of two parts, a forward and a reverse sweep. During the forward sweep, the potential is applied from a low potential value to a high potential value in a positive direction at a constant scan rate. Non-faradaic current also increases and decreased with sweeping potential. This non-faradaic current is due to the presence of electroactive functional groups on the surface of the electrode and charging of species in solution and formation of a double layer near electrode surface. Current due to the oxidation of neurotransmitter species also increases proportionally as the linear sweep reaches the oxidation potential of the species. Further increases in potential will lead to a decrease in the oxidation current due to the depletion of species near the sensing surface.

Similarly, in the reverse sweep, the potential is linearly swept from a high potential value to a low potential value at a constant scan rate. Usually, non-faradaic current is much higher than faradaic current and so to measure faradaic current, background subtraction is required. Current values at each potential of the scan are measured in the absence versus the presence of neurotransmitter, and the faradaic current is deduced by subtracting current values obtained in the presence of neurotransmitter from those detected in the absence of neurotransmitter. Typical excitation and response waveforms for a fast cyclic voltammetry experiment are shown in Figure 1.4.

Due to the sweeping potential of fast cyclic voltammetry, it is possible to distinguish between the oxidation/reduction currents of two or more species if their

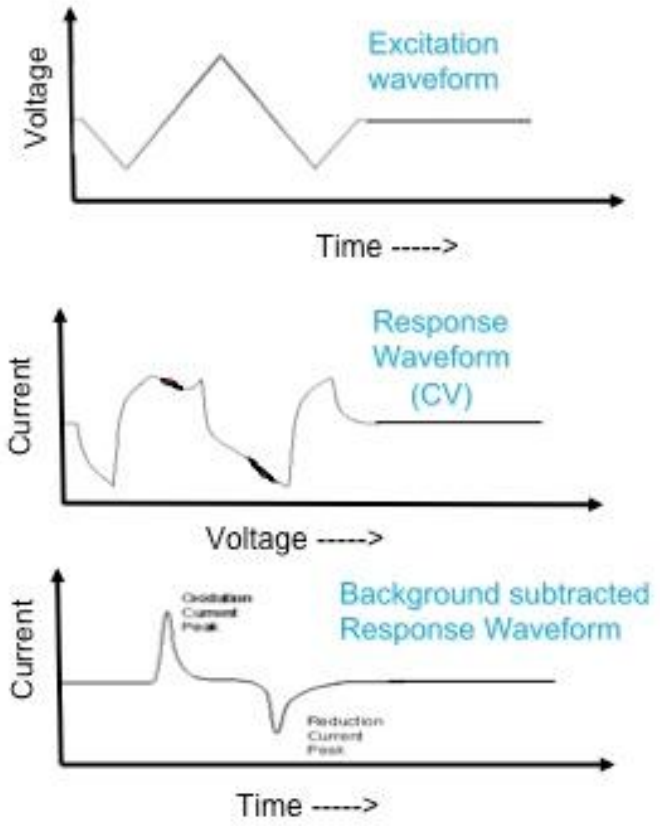

Figure 1.4: Fast cyclic voltammetry excitation and response waveforms. Typical fast cyclic waveform **(A)** consists of a positive and negative potential sweep. **(B)** Non-faradaic current due to groups on the electrode surface, ions in solution, and Hemholtz layer formation increases and decreases with potential. Faradaic current (shown in red) is most apparent near the oxidation/reduction potentials of species and usually is much smaller in comparison to background non-faradaic current. **(C)** The background subtracted current response versus voltage plot is called a cyclic voltammogram and it provides information about faradaic current responses to oxidation and reduction potentials, which are proportional, via Faraday's Law, to the concentration of the species of interest.

oxidation/reduction potentials are different. Fast cyclic voltammetry has the advantage of having greater inherent selectivity over chronoamperometry because species with different oxidation and reduction potentials can be identified based on separate oxidation and reduction peak positions (voltage) in the cyclic voltammograms. The ratio of the reductive peak current to oxidative peak current provides further information about the species being detected. Modifying the fast cyclic voltammetry waveform to exclude the oxidation/reduction potentials of interfering species can further increase selectivity. For example, the oxidation potential of serotonin comes at a slightly higher potential than dopamine or norepinephrine. Thus, changing the starting potential from -0.2 V to 0.4 V can lead to 10 times more selectivity for serotonin over dopamine (B. P. Jackson et al., 1995). One point to note is that the reductive current for serotonin is low as compared to the reductive current for other neurotransmitters. This is because after oxidation of serotonin, oxidized species of serotonin rapidly form radicals which can react with other species to form dimers or trimers, which cannot subsequently be reduced back to serotonin (M. Z. Wrona and G. Dryhurst, 1987).

1.3 Summary

The serotonergic neurotransmitter system is currently under investigation for its role in anxiety and depression. In order to understand more fully how serotonin transporter inhibition has clinical effects or how the serotonin system affects anxiety and mood disorders during development, it is necessary to have a better understanding of serotonin neurotransmission. To do so, voltammetric techniques such as chronoamperometry and fast cyclic voltammetry, were investigated. However, for

studying serotonin neurotransmission *in vivo* or *ex vivo*, more effective and reliable sensing devices and optimization of electroanalytical techniques to perform highly sensitive and selective serotonin determination are needed. In addition, placing carbon fiber microelectrodes *in vivo* causes the electrodes to be fouled, resulting in reductions in the signals sensed by the electrodes.

The goal of the research discussed in this thesis is to optimize carbon fiber microelectrodes for the voltammetric studies carried out in the Andrews' laboratory, so that more accurate and reproducible data can be collected. By creating electrodes that function with high sensitivity and selectivity and that are resistant to fouling, it will be possible to move forward and to attempt to characterize serotonergic release and reuptake rates in the mouse brain. Being able to monitor serotonin in the mouse brain will thus allow research on the serotonergic neurotransmitter system to advance.

References

1. Anderson GM, Gutknecht L, Cohen DJ, Brailly-Tabard S, Cohen JH, Ferrari P, Roubertoux PL, Tordjman S (2002) Serotonin transporter promoter variants in autism: functional effects and relationship to platelet hyperserotonemia. Mol Psychiatry 7:831-836.
2. Andrews AM (2009) Does chronic antidepressant treatment increase extracellular serotonin? Frontiers in Neuroscience 3:246-247.
3. Ansorge MS, Morelli E, Gingrich JA (2008) Inhibition of serotonin but not norepinephrine transport during development produces delayed, persistent perturbations of emotional behaviors in mice. J Neurosci 28:199-207.
4. Ansorge MS, Zhou M, Lira A, Hen R, Gingrich JA (2004) Early-life blockade of the 5-HT transporter alters emotional behavior in adult mice. Science 306:879-881.
5. Caspi A, Sugden K, Moffitt TE, Taylor A, Craig IW, Harrington H, McClay J, Mill J, Martin J, Braithwaite A, Poulton R (2003) Influence of life stress on depression: moderation by a polymorphism in the 5-HTT gene. Science 301:386-389.
6. Chaput Y, de Montigny C, Blier P (1986) Effects of a selective 5-HT reuptake blocker, citalopram, on the sensitivity of 5-HT autoreceptors: electrophysiological studies in the rat brain. Naunyn Schmiedebergs Arch Pharmacol 333:342-348.
7. Filip M, Bader M (2009) Overview on 5-HT receptors and their role in physiology and pathology of the central nervous system. Pharmacol Rep 61:761-777.
8. Frazer A (1997) Pharmacology of antidepressants. J Clin Psychopharmacol 17 Suppl 1:2S-18S.

9. Fuller RW (1994) Uptake inhibitors increase extracellular serotonin concentration measured by brain microdialysis. Life Sci 55:163-167.
10. Graeff FG (1997) Serotonergic systems. Psychiatr Clin North Am 20:723-739.
11. Greenberg BD, Tolliver TJ, Huang SJ, Li Q, Bengel D, Murphy DL (1999) Genetic variation in the serotonin transporter promoter region affects serotonin uptake in human blood platelets. Am J Med Genet 88:83-87.
12. Harvey BH (1997) The neurobiology and pharmacology of depression. A comparative overview of serotonin selective antidepressants. S Afr Med J 87:540-550, 552.
13. Heils A, Mossner R, Lesch KP (1997) The human serotonin transporter gene polymorphism--basic research and clinical implications. J Neural Transm 104:1005-1014.
14. Holmes A, Hariri AR (2003) The serotonin transporter gene-linked polymorphism and negative emotionality: placing single gene effects in the context of genetic background and environment. Genes Brain Behav 2:332-335.
15. Holmes A, Murphy DL, Crawley JN (2002) Reduced aggression in mice lacking the serotonin transporter. Psychopharmacology (Berl) 161:160-167.
16. Holmes A, Lit Q, Murphy DL, Gold E, Crawley JN (2003) Abnormal anxiety-related behavior in serotonin transporter null mutant mice: the influence of genetic background. Genes Brain Behav 2:365-380.
17. Invernizzi R, Belli S, Samanin R (1992) Citalopram's ability to increase the extracellular concentrations of serotonin in the dorsal raphe prevents the drug's effect in the frontal cortex. Brain Res 584:322-324.

18. Invernizzi R, Bramante M, Samanin R (1994) Chronic treatment with citalopram facilitates the effect of a challenge dose on cortical serotonin output: role of presynaptic 5-HT1A receptors. Eur J Pharmacol 260:243-246.
19. Jackson BP, Dietz SM, Wightman RM (1995) Fast-scan cyclic voltammetry of 5-hydroxytryptamine. Anal Chem 67:1115-1120.
20. Kandel ER, Schwartz JH, Jessell TM (2000) Principles of Neuroscience, 4th Edition. New York: McGraw Hill Professional.
21. Katzman MA (2009) Current considerations in the treatment of generalized anxiety disorder. CNS Drugs 23:103-120.
22. Kawagoe KT, Zimmerman JB, Wightman RM (1993) Principles of voltammetry and microelectrode surface states. J Neurosci Methods 48:225-240.
23. Kessler RC, Chiu WT, Demler O, Walters EE (2005a) Prevalence, severity, and comorbidity of twelve-month DSM-IV disorders in the National Comorbidity Survey Replication (NCS-R). Archives of General Psychiatry 62:617-627.
24. Kessler RC, Chiu WT, Demler O, Merikangas KR, Walters EE (2005b) Prevalence, severity, and comorbidity of 12-month DSM-IV disorders in the National Comorbidity Survey Replication. Arch Gen Psychiatry 62:617-627.
25. Leonardo ED, Hen R (2008) Anxiety as a developmental disorder. Neuropsychopharmacology 33:134-140.
26. Lesch KP, Bengel D, Heils A, Sabol SZ, Greenberg BD, Petri S, Benjamin J, Muller CR, Hamer DH, Murphy DL (1996) Association of anxiety-related traits with a

polymorphism in the serotonin transporter gene regulatory region. Science 274:1527-1531.

27. Li Q, Wichems C, Heils A, Van De Kar LD, Lesch KP, Murphy DL (1999) Reduction of 5-hydroxytryptamine (5-HT)(1A)-mediated temperature and neuroendocrine responses and 5-HT(1A) binding sites in 5-HT transporter knockout mice. J Pharmacol Exp Ther 291:999-1007.
28. Lowry CA, Hale MW, Evans AK, Heerkens J, Staub DR, Gasser PJ, Shekhar A (2008) Serotonergic systems, anxiety, and affective disorder: focus on the dorsomedial part of the dorsal raphe nucleus. Ann N Y Acad Sci 1148:86-94.
29. Mathews TA, Fedele DE, Unger EL, Lesch KP, Murphy DL, Andrews AM (2000) Effects of serotonin transporter inactivation on extracellular 5-HT levels, in vivo microdialysis recovery and MDMA induced release of serotonin and dopamine in mouse striatum. In: Society for Neuroscience.
30. Mathews TA, Fedele DE, Coppelli FM, Avila AM, Murphy DL, Andrews AM (2004) Gene dose-dependent alterations in extraneuronal serotonin but not dopamine in mice with reduced serotonin transporter expression. J Neurosci Methods 140:169-181.
31. Michael DJ, Wightman RM (1999) Electrochemical monitoring of biogenic amine neurotransmission in real time. J Pharm Biomed Anal 19:33-46.
32. Murphy DL, Campbell IC, Costa JL (1978) The brain serotonergic system in the affective disorders. Prog Neuropsychopharmacol 2:5-31.

33. Murphy DL, Aulakh CS, Garrick NA (1986) How antidepressants work: cautionary conclusions based on clinical and laboratory studies of the longer-term consequences of antidepressant drug treatment. Ciba Found Symp 123:106-125.
34. Murphy DL, Lerner A, Rudnick G, Lesch KP (2004) Serotonin transporter: gene, genetic disorders, and pharmacogenetics. Mol Interv 4:109-123.
35. Murphy DL, Andrews AM, Wichems CH, Li Q, Tohda M, Greenberg B (1998) Brain serotonin neurotransmission: an overview and update with an emphasis on serotonin subsystem heterogeneity, multiple receptors, interactions with other neurotransmitter systems, and consequent implications for understanding the actions of serotonergic drugs. J Clin Psychiatry 59 Suppl 15:4-12.
36. Murphy DL, Li Q, Engel S, Wichems C, Andrews A, Lesch KP, Uhl G (2001) Genetic perspectives on the serotonin transporter. Brain Res Bull 56:487-494.
37. Murphy DL, Fox MA, Timpano KR, Moya PR, Ren-Patterson R, Andrews AM, Holmes A, Lesch KP, Wendland JR (2008) How the serotonin story is being rewritten by new gene-based discoveries principally related to SLC6A4, the serotonin transporter gene, which functions to influence all cellular serotonin systems. Neuropharmacology 55:932-960.
38. Nestler EJ (1998) Antidepressant treatments in the 21st century. Biol Psychiatry 44:526-533.
39. Nestler EJ, Barrot M, DiLeone RJ, Eisch AJ, Gold SJ, Monteggia LM (2002) Neurobiology of depression. Neuron 34:13-25.
40. NIH (2010) Depression. In. Bethesda, MD: National Institutes of Health.

41. NIMH (2009) NIMH - The Numbers Count: Mental Disorders in America. In: National Institute of Mental Health.
42. Nolte J (2002) The Human Brain: An Introduction to Its Functional Anatomy, 5th Edition. St. Louis: Mosby, Inc.
43. Nutt DJ, Forshall S, Bell C, Rich A, Sandford J, Nash J, Argyropoulos S (1999) Mechanisms of action of selective serotonin reuptake inhibitors in the treatment of psychiatric disorders. Eur Neuropsychopharmacol 9 Suppl 3:S81-86.
44. Owens MJ, Nemeroff CB (1994) Role of serotonin in the pathophysiology of depression: focus on the serotonin transporter. Clin Chem 40:288-295.
45. Parsey RV, Hastings RS, Oquendo MA, Hu X, Goldman D, Huang YY, Simpson N, Arcement J, Huang Y, Ogden RT, Van Heertum RL, Arango V, Mann JJ (2006) Effect of a triallelic functional polymorphism of the serotonin-transporter-linked promoter region on expression of serotonin transporter in the human brain. Am J Psychiatry 163:48-51.
46. Patkar AA, Berrettini WH, Mannelli P, Gopalakrishnan R, Hoehe MR, Bilal L, Weinstein S, Vergare MJ (2004) Relationship between serotonin transporter gene polymorphisms and platelet serotonin transporter sites among African-American cocaine-dependent individuals and healthy volunteers. Psychiatr Genet 14:25-32.
47. Perry KW, Fuller RW (1992) Effect of fluoxetine on serotonin and dopamine concentration in microdialysis fluid from rat striatum. Life Sci 50:1683-1690.
48. Pineyro G, Blier P (1999) Autoregulation of serotonin neurons: role in antidepressant drug action. Pharmacol Rev 51:533-591.

49. Popa D, Lena C, Alexandre C, Adrien J (2008) Lasting syndrome of depression produced by reduction in serotonin uptake during postnatal development: evidence from sleep, stress, and behavior. J Neurosci 28:3546-3554.

50. Risch SC, Nemeroff CB (1992) Neurochemical alterations of serotonergic neuronal systems in depression. J Clin Psychiatry 53 Suppl:3-7.

51. Robinson TE, Justice JB (1991) Microdialysis in the Neurosciences. New York: Elsevier.

52. Schinka JA, Busch RM, Robichaux-Keene N (2004) A meta-analysis of the association between the serotonin transporter gene polymorphism (5-HTTLPR) and trait anxiety. Mol Psychiatry 9:197-202.

53. Sen S, Burmeister M, Ghosh D (2004) Meta-analysis of the association between a serotonin transporter promoter polymorphism (5-HTTLPR) and anxiety-related personality traits. Am J Med Genet B Neuropsychiatr Genet 127B:85-89.

54. Singh Y, Sawarynski LE, Michael HM, Ferrell RE, Murphey-Corb MA, Swain GM, Andrews AM (2009) Boron-Doped Diamond Microelectrodes Reveal Reduced Serotonin Uptake Rates in Lymphocytes from Adult Rhesus Monkeys Carrying the Short Allele of the *5-HTTLPR*. ACS Chemical Neuroscience

55. Squire LR, Bloom FE, Spitzer NC, du Lac S, Ghosh A, Berg D (2008) Fundamental Neuroscience, 3rd Edition. Canada Academic Press.

56. Wightman RM (1988) Voltammetry with Microscopic Electrodes in New Domains. Science 240:415-420.

57. Wrona MZ, Dryhurst G (1987) Oxidation chemistry of 5-hydroxytryptamine. 1. Mechanism and products formed at micromolar concentrations. J Org Chem 52:2817-2825.

Chapter 2: Electrode and waveform characterizations

2.1 Introduction and background

During neurotransmission, neurotransmitters are released from vesicles in presynaptic neurons into the synaptic cleft and the surrounding extracellular space. Neurotransmitter molecules then diffuse in the synaptic space to activate pre- and postsynaptic neurons by binding to receptors, thus relaying and propagating information from one neuron to others. Neurotransmitter released into the extracellular space either diffuses away or is taken back up by presynaptic neurons via specific transporters (D. J. Michael and R. M. Wightman, 1999; E. R. Kandel et al., 2000). Neurotransmission of biogenic amines, including serotonin, norepinephrine, and dopamine can be monitored using carbon fiber microelectrodes and voltammetry methods (R. M. Wightman, 1988).

As explained Chapter 1, in carbon fiber microelectrode voltammetry, changes in monoamine neurotransmission were determined by measuring oxidation and reduction currents produced by extracellular monoamines. According to Faraday's law, the oxidation or reduction current is directly proportional to the amount of species oxidized or reduced. Application of a voltage greater than the oxidation potential of the monoamine of interest to the carbon fiber microelectrodes leads to oxidation of monoamine (G. Dryhurst, 1990). Changes in currents generated at microelectrodes due to the oxidation/reduction of species provide information about changes in the concentrations of monoamines in the extracellular space. (R. M. Wightman, 1988; K. T. Kawagoe et al., 1993; D. J. Michael and R. M. Wightman, 1999).

The use of electrochemical techniques such as chronoamperometry and fast cyclic voltammetry have been shown to be useful for monitoring neurotransmitters *in vivo* and *ex vivo* (G. Dryhurst, 1990; K. T. Kawagoe et al., 1993; B. P. Jackson et al., 1995; D. J. Michael and R. M. Wightman, 1999), and therefore are informative for learning more about serotonin neurotransmission. However, thorough investigations of the characteristics of electrode responses and the voltage waveforms used by these techniques are required to fully understand the results of *in vivo* and *in vitro* experiments. For instance, it is necessary to characterize electrode responses via calibration with specific concentrations of neurotransmitters both before and after *in vivo* or *in vitro* neurotransmitter measurements. A reliable electrode will show a linear response to increasing concentrations of a neurotransmitter such as serotonin. An electrode that does not show a linear calibration curve should be discarded as it would not yield accurate results.

After calibrating an electrode to confirm its linear current response to increasing concentrations of a neurotransmitter, it is necessary to characterize other aspects of the electrode such as its sensitivity and selectivity for the analyte of interest. The sensitivity of an electrode refers to the ability of an electrode to show a detectable current in response to low concentrations of a given neurotransmitter. The selectivity of an electrode refers to the ability of an electrode to show high current responses to the desired neurotransmitter over other neurotransmitters and electroactive metabolites. For our experiments, ideal electrodes showed linear responses to increasing concentrations of serotonin, as well as high sensitivity and selectivity.

The sensitivity of an electrode for a neurotransmitter is dependent on the geometry, size, and properties of the exposed surface of the electrode (R. M. Wightman, 1988). The size and shape of the exposed surface of an electrode affects its sensitivity and background noise. In experiments described throughout this thesis, several different carbon fiber electrode geometries were employed, including cylindrical, "blunt cut" (flat, circular surface), and beveled (elliptical surface). If the surface of the electrode used in an experiment is too large, the electrode will show high a background current, thus making it unusable due to the low signal-to-background ratios. While the limits of detection of the instrument could theoretically be extended by modifications to the system, this would not change the signal to background ratio. An appropriate electrode shape and size must thus be found. To be able to make accurate measurements of serotonin *in vivo* or *ex vivo*, it is thus necessary to find a balance between the appropriate electrode shape and size.

As mentioned previously, the ability of an electrode to be selective is important, particularly when attempting to make voltammetric measurements in an environment that contains many different electroactive neurotransmitters and metabolites. Apart from variations in the current responses of electrodes to different neurotransmitters, selective determination of a neurotransmitter can also be achieved by monitoring oxidation and reduction potentials and using the ratio of the reduction current to the oxidation current (redox ratio), which is somewhat characteristic of individual species. For example the redox ratios of dopamine, norepinephrine, and serotonin measured during well-plate chronoamperometric calibration are 0.7±0.05, 0.7±0.01, and 0.2±0.03,

respectively. In constant potential amperometry and high-speed chronoamperometry in which the exact oxidation or reduction potentials cannot be monitored due to the stepped application of the voltage, redox ratios can be an important factor for determining the species that was oxidized or reduced. For example, the oxidation products of serotonin are unstable and form dimers, thus decreasing the concentration of species available for reduction, while dopamine and norepinephrine do not show this behavior (M. Z. Wrona and G. Dryhurst, 1987). Therefore the redox ratio of serotonin is significantly lower than that of dopamine and norepinephrine thus making it easier to distinguish serotonin.

In addition to characterizing electrode responses to commonly used waveforms, it is also necessary to understand the effects that varying the applied waveform have on electrode responses. In both chronoamperometry and fast cyclic voltammetry, altering the shape of the applied waveform, the voltage limits of the applied voltage waveform, and chemical pretreatments of the electrodes can change the sensitivity and selectivity of the electrodes. In order to maximize sensitivity and selectivity of carbon fiber microelectrodes for serotonin detection, waveform characterization experiments were performed by changing resting and applied potentials in chronoamperometry or the shape of the waveform and scan rate in fast cyclic voltammetry. Additionally, the effects of pretreatments on the current responses of carbon fiber microelectrodes during chronoamperometry were also investigated. The purpose of these experiments was to find improved waveforms and electrode pretreatments for sensitive and selective serotonin detection.

For *in vivo* experiments, it is also important to understand how electrode responses change over time after being in contact with biological tissues. The responses of carbon fiber microelectrodes upon exposure to biological tissues changes over time due to adsorption of biological macromolecules on the electrode sensing surfaces, thus fouling the electrodes and leading to variable and reduced sensitivity (N. Wisniewski and M. Reichert, 2000). Different resting and applied voltages were used to study the effects of different waveforms on electrode fouling. Additionally, electrode pretreatments were investigated for their abilities to prevent electrode fouling.

2.2 Materials and methods

2.2.1 Electrode fabrication

The electrodes that were designed and created for the voltammetric experiments described in the following sections were of central importance to the completion of these experiments. The microelectrode fabrication process requires skill and precision. The ability to fabricate reproducibly sensitive and selective microelectrodes was acquired after months of practice. It is recommended that the following protocols be followed closely to achieve optimal results.

Cylindrical CFMs (30 µm)

The most commonly used type of electrode used in the experiments performed in the following sections was a 30 µm carbon fiber electrode. These electrodes were used in the great majority of the *in vitro* chronoamperometry experiments.

Carbon fiber (30-µm) was purchased from Amoco (Greenville, SC) on a cylindrical roll (continuous single fiber). A single carbon fiber was wound off the roll and cut to a length of 12-13 cm. In order to remove strands or extraneous material, the carbon fiber was gently brushed along its length several times while holding one end of the carbon fiber on a flat, clean surface with one finger. Cleaned, single carbon fibers of the desired length were aspirated singly into 10 cm long borosilicate glass capillary tubes with an outer diameter of 1.2 mm and an inner diameter of 0.60 mm (Sutter Instruments, Novato, CA). An aspiration system was set up using a vacuum line in the lab, rubber tubing, a plastic T-joint, and a Pasteur pipette rubber bulb. One end of the rubber tubing was connected to the vacuum line and the other to the T-joint. A small hole was created in the top of the rubber bulb, while the other end of the bulb was connected to the T-joint. A glass capillary was inserted into the hole in the rubber bulb. The vacuum line was opened and while holding down one end of the carbon fiber strand, the aspirator was closed off at the remaining T-joint opening using a finger of the opposite hand to induce suction through the capillary tube. The vacuum pressure was then used to insert the length of the carbon fiber into the capillary. Once the carbon fiber was visible from both ends of capillary, the suction on the aspirator was released and the capillary tube was gently pulled out of the rubber bulb. If excess carbon fiber protruded from either end of the capillary, the carbon fiber was trimmed using small scissors.

The next step in the microelectrode fabrication process was pulling the carbon fiber-inserted capillary using a P-97 electrode puller (Sutter Instruments, Novato, CA). The capillary with the carbon fiber inside was pulled from both sides while heating in

the middle. The carbon fiber protruding from the pulled end of the capillary was cut using small scissors as close to heated end of the pulled electrode as possible. This led to the formation of two microelectrodes with cylindrical carbon fiber exposed at one end, tightly encapsulated in glass capillary. The exposed carbon fiber was further trimmed using a scalpel under a light microscope so that the length of carbon fiber protruding from the tip of the glass-carbon fiber junction was between 200-300 μm. The electrode puller was calibrated prior to use by pulling an empty capillary and noting the necessary effective pulling temperature. To insure a tight fit between the pulled glass capillary and the carbon fiber, 10-15 units higher temperature than what was needed to pull an empty capillary was used. Other settings used for optimal performance of the electrode puller were as follows: Pull = 70, Velocity = 100.

The pulled and trimmed electrodes were then coated with a layer of epoxy. Three 20 mL vials with lids were filled with isopropanol, acetone, and epoxy respectively. The vials were appropriately labeled with the contents and date. The vial containing epoxy was used immediately and discarded after 10 min. In order to create the epoxy solution, it was necessary to use a 4:1 mixture of A:B epoxy solutions (Epo-tek, Billerica, MA). Twelve grams of solution A was mixed with 3 g of solution B in the 20 ml vial to create a volume of epoxy solution in which to place the electrodes. Once epoxy A and B were added, the solution was stirred using a plastic disposable pipette for one minute.

Electrodes were carefully grouped together by holding the electrodes and arranging them so that their carbon fiber tips were all at the same level. Approximately 10-13 electrodes could be dipped in one group. A large binder clip with cushioning Kimwipes or paper folded inside was used to clamp the group of electrodes together. Each group of electrodes was immersed into the isopropanol for one to three minutes to a depth that allowed the entire exposed carbon fiber to be surrounded by isopropanol, followed by five minutes of drying in air. Afterward, the batch of electrodes was placed into the epoxy solution for seven minutes. Afterwards, the batch of electrodes was very carefully dipped into the acetone solution for a few seconds. Only one or two millimeters of the electrode tips were submerged in the acetone solution. The goal of dipping the electrodes into epoxy was to create an insulated seal between the carbon fiber and the pulled glass capillary, and in addition, to cover a portion of the exposed carbon-fiber surface. The purpose of dipping the tips of the electrodes into the acetone was to remove epoxy and expose only a small portion of the carbon fiber. The exposed carbon fiber acts as the sensor, which detects the presence of serotonin in solution(s). This process was repeated until whole batches of electrodes (between 50-100 electrodes) were cleaned with isopropanol, coated with epoxy, and their tips uncoated by exposure to acetone.

The electrodes were then placed in an oven set to between 100 and 120 °C for 24 to 72 hours. After curing, the electrodes were taken to the microscope and were trimmed using 20X magnification with a scalpel. When looking at the electrodes under the microscope, it was necessary to recognize both where the pulled glass capillary

ended and where the epoxy coating ended. The point at which the epoxy coating ended was considered the origin from which the bare carbon fiber was measured. The exposed carbon fiber of each electrode was then trimmed to a length of 80 to 150 µm from the origin.

Cylindrical CFMs (5 µm)

The 5 µm cylindrical CFMs were fabricated in a similar manner to the 30 µm cylindrical CFMs, discussed above. However, the techniques used to make the 5 µm CFMs were more delicate, since 5-µm carbon fibers break more easily. Five-micron diameter carbon fiber was obtained from Thornel Carbon Fiber (Woodland Park, NJ) and lengths of 20 cm of the woven carbon fiber were cut from the main roll. The cut carbon fiber was then placed into a folded piece of paper, and the different threads of 5-µm carbon fiber were gently teased out of the woven piece of carbon fiber. Individual strands of carbon fiber were lightly pulled out on the piece of folded paper to aid in visualizing these thin fibers. When a strand of carbon fiber was long enough to be inserted into a borosilicate glass capillary tube, one finger was lightly dragged along its length to ensure that only a single carbon fiber was to be used and inserted into the tube.

The aspiration procedures for inserting 5-µm carbon fiber into glass capillaries were the same as those for the 30-µm microelectrodes. In addition, the capillary pulling, isopropanol cleaning, epoxy coating, acetone coatings, and oven procedures were identical for the 5 µm CFMs. In order to trim the exposed carbon fiber to the

appropriate length (again, between 80 and 150 µm in length), a greater amount of precision was needed when using the microscope and scalpel. It is easier to break the carbon fiber by accident and it is more difficult to visualize the appropriate origin (where the bare carbon fiber begins and the epoxy coating ends) in the case of 5-µm carbon fiber electrodes.

Beveled CFMs (30 µm)

Fabrication protocols for 30-µm beveled CFMs were similar to those of the 30-µm cylindrical electrodes with the exception of the last few steps. The electrodes were pulled using the P-97 puller, cleaned with isopropanol, and coated with epoxy. Instead of exposing the tips of the epoxy-coated electrode to acetone, the epoxy-coated electrodes were cured straight away in an oven at 100-120 ^{o}C for 24 to 72 h. The electrodes were examined to make sure there was at least 50 µm of carbon fiber epoxy-coated tip extending from the glass capillary. If the glass capillary was too close to the tip of the electrode, the electrode was discarded, as it would scratch the beveller.

In order to bevel the electrodes, the beveller (Sutter Instruments, Novato, CA) was disassembled and oil was placed onto the interface between the rotating pedestal and the disk (104D grit values). The disk was affixed to the pedestal and a layer of water from a squirt bottle was carefully placed onto the top of the disk. After this, an electrode was placed in the electrode holder at a 45° angle from the plane of the rotating disk. It was essential that the electrode be positioned so that it was not pointing directly at the rotating disk. This would break the electrode and scratch the beveling

disk. The electrode was slowly lowered into the water on top of the rotating disk and then carefully lowered further until the electrode touched the surface of the disk. It was sometimes necessary to lower the electrode slightly further than the point at which the electrode and the rotating disk just touch, in order for beveling to sufficiently occur.

The beveller was allowed to rotate for approximately 10 minutes followed by examination under the light microscope to observe the beveled surface. If the exposed electrode surface was not properly beveled, the electrode was moved lower and beveled for additional 10 minutes.

Reference electrodes

Reference electrodes were created and used for all of the voltammetry experiments discussed in this thesis. The purpose of these electrodes is to provide a reference for the working electrode (carbon fiber microelectrodes). Reference electrodes have established and invariant electrode potentials. In electroanalytical measurements, when it is necessary to change the potential at your working electrode, it is necessary to use a reference electrode. Due to the invariant nature of the reference electrode, its potential remains practically unchanged during the application of a potential on the working electrode, and thus, the potential at the working electrode can be measured relative to reference electrode.

Reference electrodes for the experiments described below were Ag-AgCl electrodes that were created using electroplating techniques. In order to create reference electrodes, a 1 to 1.5 inch long piece of silver wire was placed in 3 M HCl

solution and attached to one side of a 9 V battery. Another silver wire was attached to the other side of the battery and placed into the HCl solution. After a period of about 5-10 min, electroplating was complete and the Ag-AgCl reference electrode was ready for use in experiments.

2.2.2 *Ex vivo* chronoamperometry procedures

In order to perform chronoamperometric experiments, an excitation waveform (square wave) was applied to the working electrode. The electroactive species of interest (in our case, serotonin) were oxidized during the oxidation step, and the oxidized species were then reduced during reduction step of the applied waveform. Because of the oxidation or reduction of the species in solution, electrons were either gained by the electrode (oxidation) or lost into solution (reduction). Changes in the current values at the working electrode surfaces due to these processes were monitored by the instrument. The current responses of electrodes to various concentrations of neurotransmitter species were used to construct calibration curves. Calibration curves were used in *in vivo* or *ex vivo* experiments with the same electrode to measure changes in the concentrations of neurotransmitters in the biological system.

Set up parameters

Chronoamperometry experiments were performed using the Tar Heel CV program and data were analyzed using ChronoAmp, a custom designed program written by Yogesh Singh. For standard chronoamperometry experiments, the Tar Heel CV program was opened and parameters were adjusted to the specifications listed below.

Parameters not mentioned as needing to be adjusted were not altered (standard settings on the Tar Heel CV program were used). After opening the Tar Heel CV program, “Create Waveform” was selected, and a step waveform was created by designating the first three formulas for the potential values as y=0, y=0.55, and y=0 for 0.1 seconds each, unless otherwise specified. This creates a three-step waveform where each step is 100 ms long. The first step with the potential at 0 V was used to monitor changes in background current, while the second and third steps were used to monitor oxidation and reduction currents, respectively. All other formulas were removed from consideration by entering their applied time as 0 s. The multiplier value was set to 1.00. Next, the “Evaluate” button and the “Use Waveform” buttons were selected to apply the changes that were made. The waveform application frequency was changed to 1.00 Hz, and the “Apply Waveform” switch was turned on in the Tar Heel CV program.

For chronoamperometry experiments in a 12-well plate, the working and reference electrodes were lowered into the solution in a single well and using the oscilloscope function of the Tar Heel CV software, a current versus voltage profile was observed to assess whether the electrodes were working properly. To collect background or experimental data, the “Total Time (s)” was set to the amount of time the data was to be recorded. Finally, “Collect Data” was selected from the main menu in the Tar Heel CV program and the appropriate file was chosen to store the data. A representative current false color three-dimensional plot of a chronoamperometric calibration experiment and a current versus time curve for a single scan is shown in Figure 2.1 below.

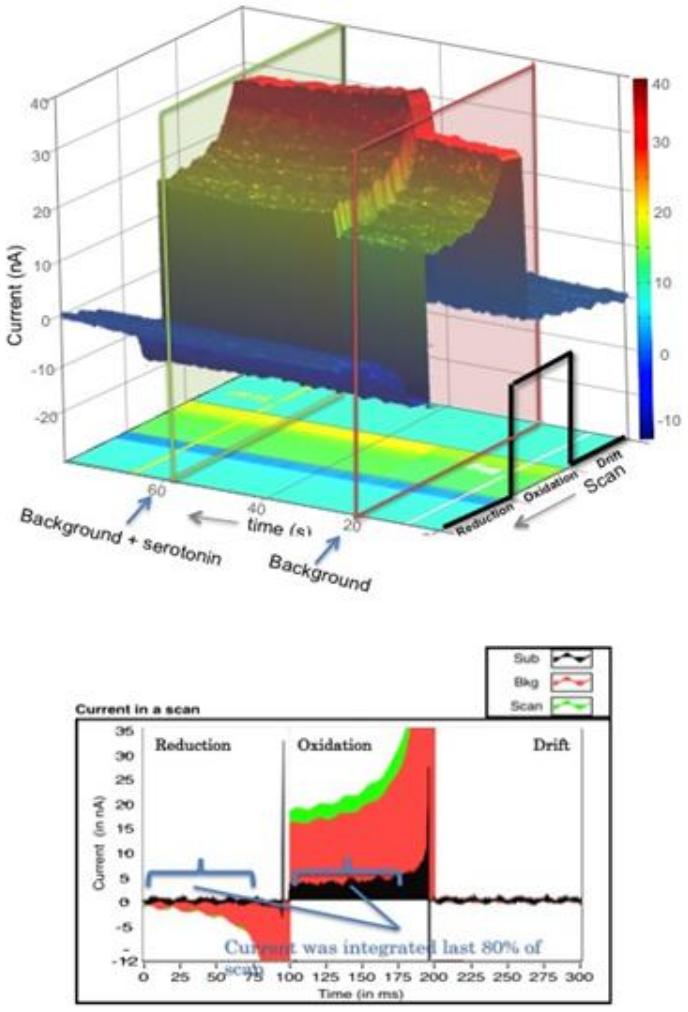

Figure 2.1: Representative chronoamperometric current profiles. The top figure shows a three-dimensional current profile of a chronoamperometric calibration experiment. 1 µM serotonin was injected at time=30 seconds. In the bottom figure, a current versus time plot of background (red) and background + serotonin (green) are shown in two-dimensions. The difference between the scan (background +serotonin) and background curves gives a resultant subtracted current due to serotonin only and is shown in black. The portion of the curve from 0 to 100 ms is representative of the background information when a voltage of 0 V is applied. From 100 to 200 ms, the oxidation portion of the scan occurs, and from 200 to 300 ms, the reduction portion of the scan can be seen.

The data collected in the last 80% of scans of each step were integrated. The integrated current was background subtracted and the background subtracted integrated current versus time plot was used to give information about faradaic oxidation and reduction currents.

2.2.3 *In vivo* fast cyclic voltammetry procedures

Similar to the chronoamperometry method, in fast cyclic voltammetry, electrode responses must be calibrated for various concentrations of neurotransmitters prior to the actual experiment. Fast cyclic voltammetry techniques were used with 5-μm carbon fiber microelectrodes. Due to the small sensing area, it is not advisable to expose the electrode to a neurotransmitter like serotonin for long periods of time since this causes electrode fouling. Thus, a flow-injection set up was used for the electrode calibration experiments. In the flow-injection set up, electrodes were in contact with neurotransmitter for small amount of time (2-3 seconds).

Set up parameters

Fast cyclic voltammetry experiments were performed using the Tar Heel CV program and the data were analyzed using a custom FCV program designed in house. For standard fast cyclic voltammetry experiments, the Tar Heel CV program was opened and the parameters were adjusted to the specifications listed. Parameters not mentioned as needing to be adjusted were not altered (standard settings on the Tar Heel CV program were used). After opening the Tar Heel CV program, the “Create Waveform” button was selected and a sweep waveform was created using these

settings, unless otherwise specified: starting potential -0.4 V, ending potential 1.3 V and a scan rate of 400 V/s. The multiplier value was set to 1.00. Next, the “Evaluate” button and the “Use Waveform” buttons were selected to apply the changes that were made. The waveform application frequency was changed to 10.0 Hz, and the “Apply Waveform” switch was turned on in the Tar Heel CV program. A false color three-dimensional plot of an electrode calibration experiment and a representative current versus voltage (cyclic voltammogram) and current versus time plot are shown in Figure 2.2, below.

A schematic of the flow cell set-up used in the fast cyclic voltammetry experiments is shown in Figure 2.3. The buffer used in these experiments was a 1x PBS-aCSF (2.68 mM KCl, 136.8 mM NaCl, 1.23 mM $MgCl_2.H_2O$, 1.19 mM $CaCl_2 \cdot 2H_2O$, 10.14 mM Na_2HPO_4, and 1.76 mM KH_2PO_4). A buffer flow rate of 3.0 mL/min was maintained using a peristaltic pump (Peristar Pro, World Precision Instruments, Sarasota, FL). Switching the flow path from buffer to a neurotransmitter solution was achieved using a Rheodyne valve (Valco Instruments Company, Houston, TX). In the inject mode, the neurotransmitter solution merges into the flow path of the buffer and flows toward the electrode in the flow cell, ultimately exiting to the reservoir. Because of the constant flow rate used in these flow cell experiments, the electrode was in contact with neurotransmitter solution for a short period of time of only 3-4 seconds, thus minimizing the risk of electrode fouling due to exposure to neurotransmitter.

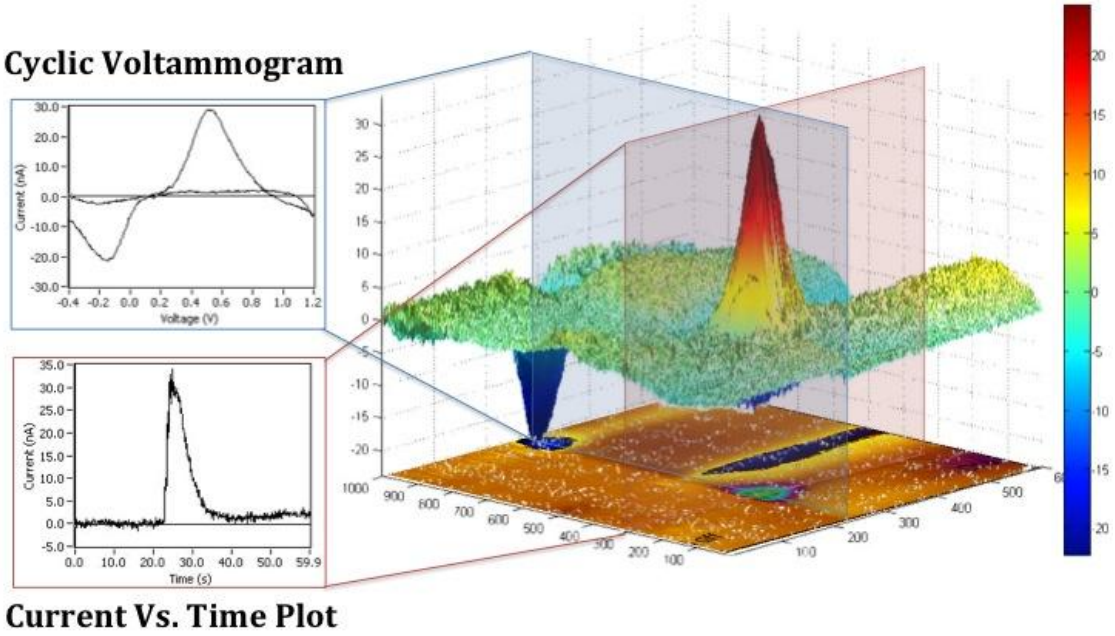

Figure 2.2: Representative fast cyclic voltammetry current profiles. A false color three-dimensional current profile of a fast cyclic voltammetry experiment is shown on the right. Current values are shown as color on the z-axis. Dopamine (1 µM) was injected at time t=20 s. The slice on the time scale when dopamine is in contact with electrode (blue plane) shows the current versus voltage (cyclic voltammogram) curve. The peak oxidation and reduction potential values in the cyclic voltammogram provide distinctive information about the species being studied. The slice on the voltage scale at the peak oxidation potential gives the oxidation current versus time plot (red plane). A sharp rise and drop in oxidation current with the baseline current returning to zero when dopamine exits the flow cell indicates proper functioning of electrodes and the flow-cell set-up.

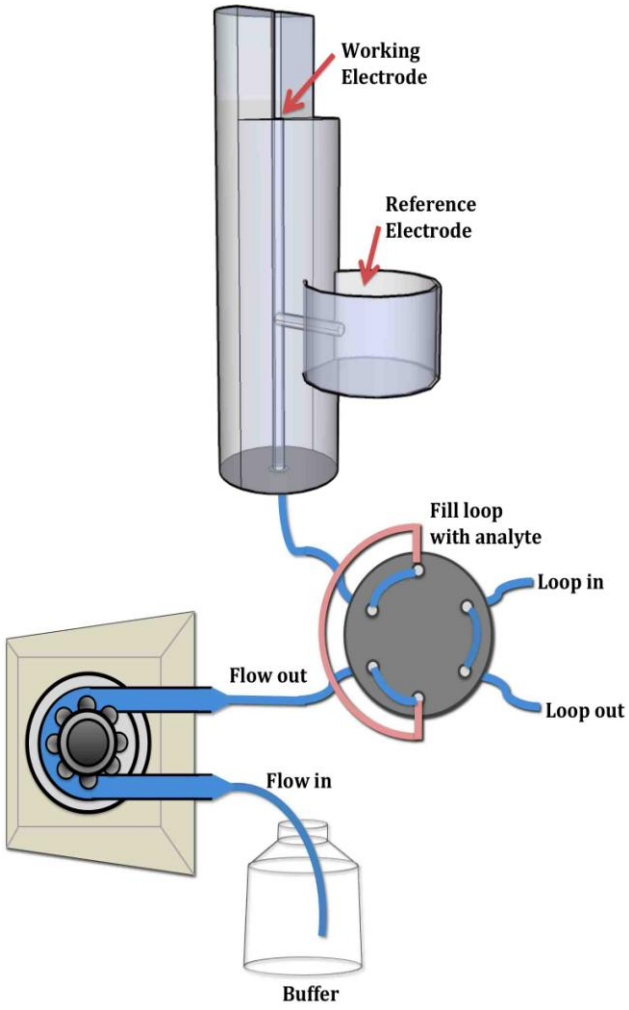

Figure 2.3: Flow cell set-up. The custom flow cell used in these experiments was set up as shown in the schematic above. Buffer was pumped (at controllable rates) through a large tube that entered the flow cell chamber. Solutions containing the neurotransmitter of interest could be pumped into the loop and then injected into the flow cell when the loop with neurotransmitter was switch into flow path using the Rheodyne valve. This flow injection set-up allowed electrode calibration without exposing the working electrode to neurotransmitter for long periods of time.

2.2.4 Chemicals

Serotonin, norepinephrine, dopamine, Nafion, isopropanol, and epoxy were purchased from Sigma-Aldrich (St. Louis, MO). All chemicals used for the assay buffer preparation were purchased from VWR (West Chester, PA).

2.2.5 Data analysis and statistics

Data comparing two means were analyzed using two-tailed unpaired *t*-tests. One-way analysis of variance (ANOVA) was used in cases where more than two means were compared, followed by either Tukey's *post hoc* tests or *t*-tests. Calibration data were analyzed by linear regression. All statistical analyses were performed using Graph-Pad Prism v.4 for Mac (GraphPad Software, La Jolla, CA). All values are expressed as means ± standard errors of the mean (SEMs), with differences of $P<0.05$ considered statistically significant. Significant differences are denoted in the figures as $*P<0.05$, $**P<0.01$, and $***P<0.001$.

2.3 Results

In depth analyses of the voltammetric properties and response characteristics of 30-µm carbon fiber microelectrodes were performed using chronoamperometry and fast cyclic voltammetry. To perform biological experiments using these electrodes, it was necessary to understand their normal response characteristics. Here, the sensitivity, selectivity, and fouling responses of carbon fiber microelectrodes were investigated.

2.3.1 Electrode calibration using chronoamperometry in well plates

Before performing experiments with 30-μm carbon fiber microelectrodes, electrodes were calibrated against known concentrations of neurotransmitters. Electrodes show changes in current in response to the addition of a neurotransmitter due to the oxidation or reduction of neurotransmitters. If an electrode was fabricated correctly, the current response to changes in neurotransmitter concentration will be linear in nature (in the concentration range of μM). By performing serial calibrations so that the concentration of serotonin increases in known increments and measuring the changes in current in response to various concentrations, a calibration curve can be created. Integrative current versus time plots of well-plate calibration experiments of various neurotransmitters are shown in Figure 2.4. In Figure 2.5, the calibration curves generated for electrodes based on integrative current versus time plots shown in Figure 2.4 for serotonin, dopamine and norepinephrine are shown. Redox ratios of the various transmitters can be determined from these data.

2.3.2 Electrode responses to various neurotransmitters

While serotonin is the primary neurotransmitter of interest in these investigations, it is certainly not the only neurotransmitter found in the brain. Therefore, when inserting carbon fiber microelectrodes into the brain, the electrode must be able to detect and to detect one specific type of neurotransmitter over another. The ability of microelectrodes to discern between several types of neurotransmitters to measure effectively only one neurotransmitter (in our case, serotonin) is termed selectivity.

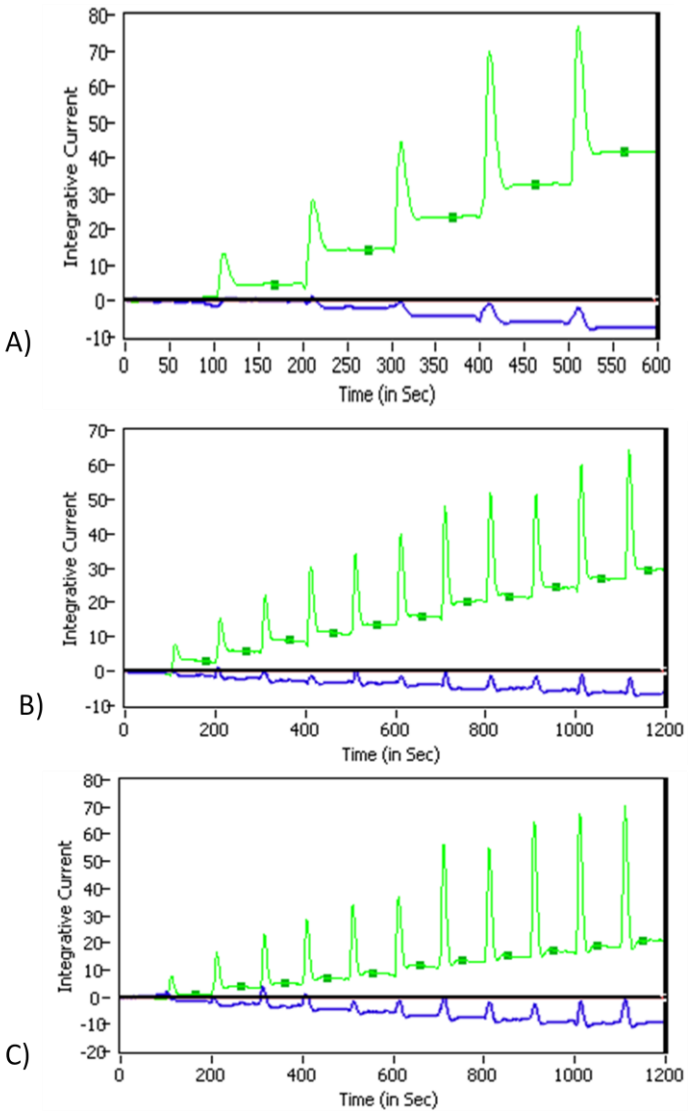

Figure 2.4: Current vs. time plots for chronoamperometric calibration experiments performed in 12-well plates for various monoamine neurotransmitters. Representative Integrated current versus time curves for A) serotonin, B) dopamine, and C) norepinephrine. The figure shows representative serial calibrations during a chronoamperometry calibration experiment in a well-plate. Neurotransmitters are incrementally added in small volumes of neurotransmitter (200 nM increments for serotonin, 100 nM increments for dopamine and norepinephrine) to the same well followed by stirring for 2-3 seconds. The current increases linearly with increasing concentrations of the neurotransmitters in the well. The peaks seen immediately after each addition of neurotransmitter are due to stirring. Current responses to the concentration of neurotransmitters were measured 30 s after stirring (shown by square shaped-points on the green oxidation current curves) to avoid changes in current values due to stirring. Reduction currents are shown in blue.

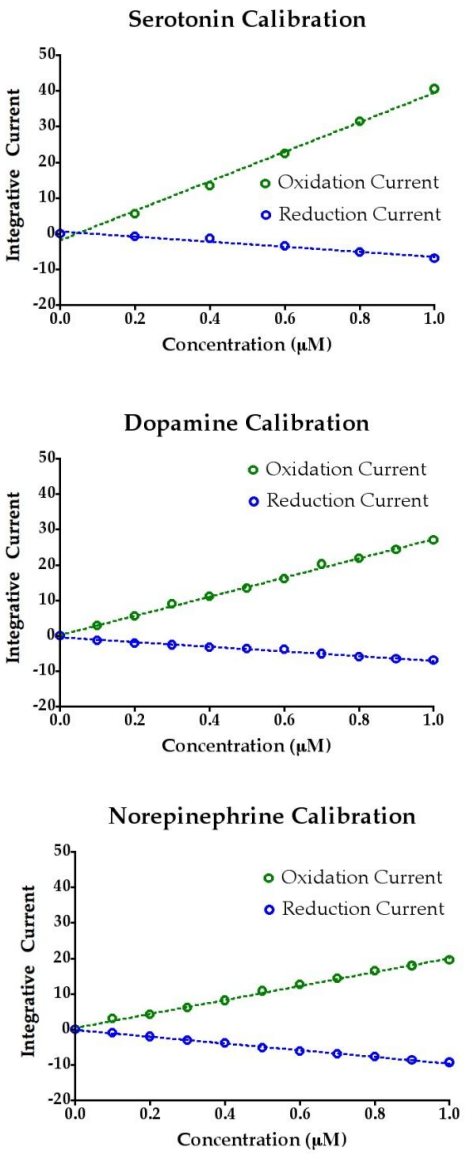

Figure 2.5: Chronoamperometric calibration curves of monoamine neurotransmitters. Representative calibration curves for A) serotonin, B) dopamine, and C) norepinephrine are shown**.** Integrative current versus concentration curves (calibration curve) shown here serve dual purposes of calibrating changes in current with respect to concentration of each neurotransmitter and determining sensitivity, which is reflected in the slope of the calibration curves. The steeper the slope, the more sensitive the electrode is to detecting the neurotransmitters. As can be seen in this figure, both the oxidative (green) and the reductive (blue) currents show highly linear responses in the 100 nM to 1000 nM concentration ranges for all three neurotransmitters. The serotonin oxidative and reductive currents showed linear responses to changes in serotonin concentration, r^2=0.9940 and r^2=0.9638, respectively. Norepinephrine showed a linear response for changes in oxidative current, r^2=0.9976, and reductive current, r^2=0.9823. Dopamine also showed a linear response for both oxidative and reductive currents in response to changes in dopamine concentration, r^2=0.9963 and r^2=0.9959, respectively.

As discussed above, chronoamperometry techniques have moderate selectivity because we can determine redox ratios for different neurotransmitters. Determining the redox ratio seen by an electrode in response to different neurotransmitters can help to identify whether the monitored current is due to one neurotransmitter over another. The redox ratio is calculated as the ratio of the reductive current to the oxidative current. Figure 2.6 shows that the current due to serotonin can be identified because the redox ratio for serotonin was significantly less than that of dopamine or norepinephrine.

2.3.3 Optimizing electrode sensitivity

Here, we investigated various parameters to determine optimal conditions under which CFMs could detect low concentrations of serotonin. To do this, we first determined the optimal resting and oxidation potentials to be used in chronoamperometry experiments. Our goal in these experiments was to determine the best potential settings to use in chronoamperometry to make future experiments as sensitive for serotonin as possible. Additionally, we looked into several possible electrode pre-treatment methods that could enhance the overall sensitivity of CFMs in chronoamperometry experiments.

Optimizing resting potentials

To improve the settings used for the application of the resting and oxidation potentials in chronoamperometry, several sets of experiments were performed in which the resting and oxidation potentials were altered and the oxidation current was

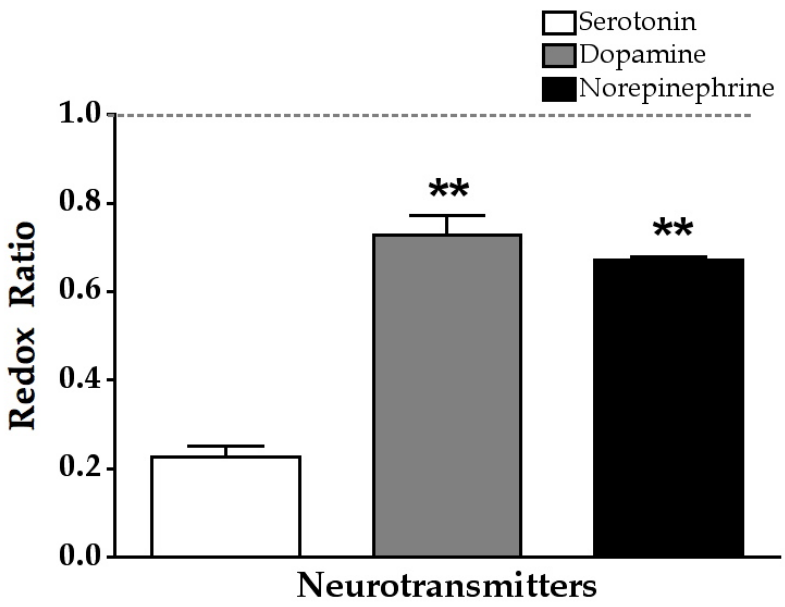

Figure 2.6: Comparison of redox ratios of monoamines using chronoamperometry. One way of identifying serotonin is by calculating redox ratios. The redox ratio for serotonin is significantly less [$F(2,24)=63.72$, $P<0.0001$] than that of dopamine and norepinephrine because the oxidation products of serotonin dimerize and undergo other side reactions such that reversible reduction cannot efficiently occur. Redox ratios of dopamine and norepinephrine are not significantly different and thus they cannot be distinguished from one another in mixtures using chronoamperometry. This gives us moderate selectivity for serotonin over dopamine and norepinephrine in chronoamperometry experiments using carbon fiber electrodes. Numbers of electrodes are: n=10 for serotonin, n=11 for dopamine, n=6 for norepinephrine. All values are expressed as means ± standard errors of the mean (SEMs), with differences of $P<0.05$ considered statistically significant. Significant differences are $^{**}P<0.01$ compared to serotonin redox ratio.

measured. For the experiments used to determine the optimal resting potential, the oxidation potential was held constant at 0.55 V, while the resting potential was reduced from 0.0 V, to -0.1, -0.2, and -0.3 V.

The oxidative current at each of these different resting potentials was measured after injections of 500 nM serotonin. As seen in Figure 2.7, decreasing the applied resting potential increases the oxidative current produced at the working electrode as compared to the case of a 0.0 V resting potential. Tukey's-*post hoc* test suggested the saturation of electrode response after decreasing the resting potential to -0.2 V, as the current response for the -0.2 V resting potential and -0.3 V resting potential were not significantly different. This suggested that the -0.2 V resting potential was a better choice than using the conventional 0.0 V resting potential due to increased electrode sensitivity as reflected by greater oxidative current responses to the same concentrations of serotonin.

Optimizing oxidation potentials

In addition to testing how changes in the applied resting potential affect electrode sensitivity, we also characterized how increasing the oxidation potential altered electrode sensitivity. The resting potential of the electrodes was held constant at 0.0 V and the applied potential was incrementally varied from 0.3 to 0.7 V. The oxidative current was measured in each experiment for a given concentration of serotonin (500 nM). Figure 2.8 shows the results from this experiment on electrode sensitivity characterization. Here, the baseline condition was considered to be the applied

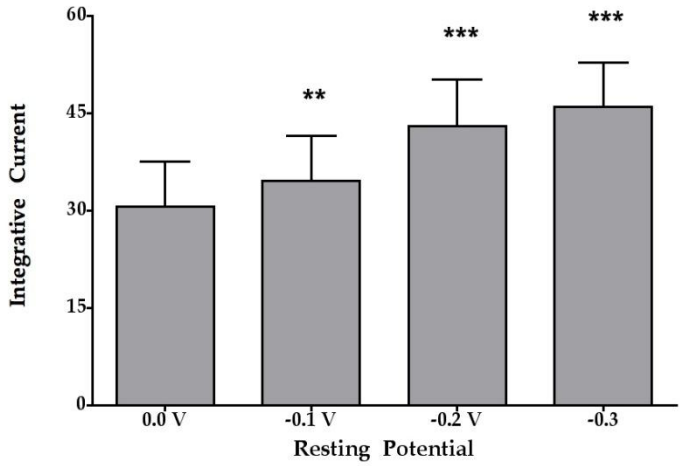

Figure 2.7: Analysis of resting potential determinations. This figure shows the changes in oxidative currents seen at different resting potentials. Decreasing the resting potential from 0.0 V significantly increases the oxidative current [$F(8,5)=15$, $P<0.0001$]. N=9 for all resting potential values. All values are expressed as means ± standard errors of the mean (SEMs), with differences of $P<0.05$ considered statistically significant. Significant differences are $^{**}P<0.01$ and $^{***}P<0.001$ compared to 0.0 V resting potential.

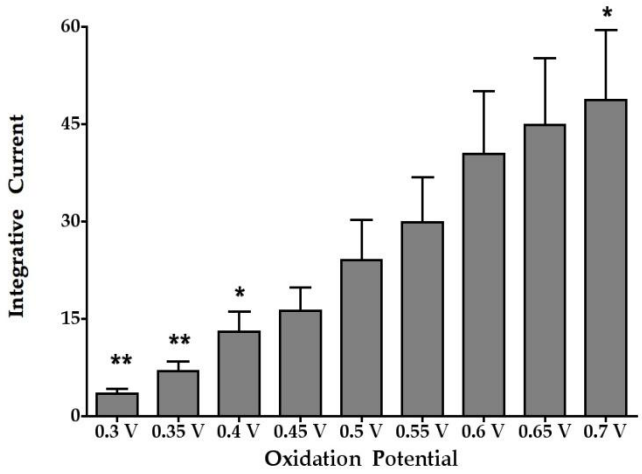

Figure 2.8: Analysis of optimal oxidation potential. These data were collected by holding the resting potential constant at 0.0 V and changing the oxidation potential. The oxidative current was determined for each oxidation potential. We observed a significant decrease in electrode sensitivity for oxidation potential values lower then 0.4 and saw a significant increase in electrode sensitivity for a 0.7 V oxidation potential value [$F(3,8)=89$, $P<0.0001$]. N=6 for all oxidation potentials. All values are expressed as means ± standard errors of the mean (SEMs), with differences of $P<0.05$ considered statistically significant. Significant differences are denoted as $*P<0.05$ and $**P<0.01$ compared to 0.55 V oxidation potential.

potential of 0.55 V, since this is the applied potential most frequently used in past experiments (X. A. Perez and A. M. Andrews, 2005; X. A. Perez et al., 2006). As seen in Figure 2.8, increasing the applied potential resulted in a significant increase in oxidation current for only the 0.7 V oxidation potential value. On the other hand, we observed a significant decrease in oxidation current for oxidation potential values lower than 0.4 V. However, we did not observe saturation of the current response with increasing potential, thus indicating additional higher voltage measurements are required for identifying the optimal oxidation potential. Based on these results we can conclude that maximal current response and thus, the highest electrode sensitivity was observed for a 0.7 V oxidation potential value over the range tested here.

Electrode pretreatments

Experiments were performed to investigate the effects of various treatments applied to electrodes prior to their use on electrode sensitivity. Four different pre-treatments were investigated. The first pre-treatment was an extended waveform with a voltage potential range from -0.3 to 0.8 V. The second pre-treatment was a cleaning waveform with an applied voltage range of +/- 1.8 V at a frequency of 30 Hz for 30 seconds. The third pre-treatment was an isopropanol cleaning protocol that involved immersing electrodes in isopropanol for 30 seconds and then air-drying before performing experiments. The fourth and last treatment involved treating electrodes with a Nafion polymer to deposit a perfluorinated ion-exchange resin on the carbon

fiber surfaces using a protocol previously described (G. A. Gerhardt and A. F. Hoffman, 2001).

Untreated electrodes were used as the control in this case and data were measured as percent change in sensitivity after each treatment compared to the response observed with untreated electrodes. The results of this pretreatment experiment are shown in Figure 2.9, and they reveal that with the exception of the isopropanol treatment, all treatments (extended waveform, cleaning waveform, and Nafion coating) showed significant increases in electrode sensitivity.

2.3.4 Effects of electrode fouling

During the process calibration or actual experiments, fouling of the electrodes can occur. In *in vitro* experiments, oxidized serotonin can adsorb to the surface of carbon fiber microelectrodes. *In vivo* experiments also result in electrode fouling due to adsorption of oxidized serotonin. However, there are also many other neurotransmitters and chemical species that can adsorb to the surfaces of the electrodes. In addition, *in vivo* experiments have the added factor of exposure to proteins and other biomolecules, which also adsorb to the surfaces of the electrodes. The adsorption of all of these species prevents or interferes with electrode sensing capabilities. This adsorption and thus, loss in electrode sensitivity, is referred to as electrode fouling. In this project, we investigated carbon fiber microelectrode fouling due to high concentrations of serotonin (10 μM) using chronoamperometry. Changes in electrode sensitivity after fouling were measured using a conventional waveform and

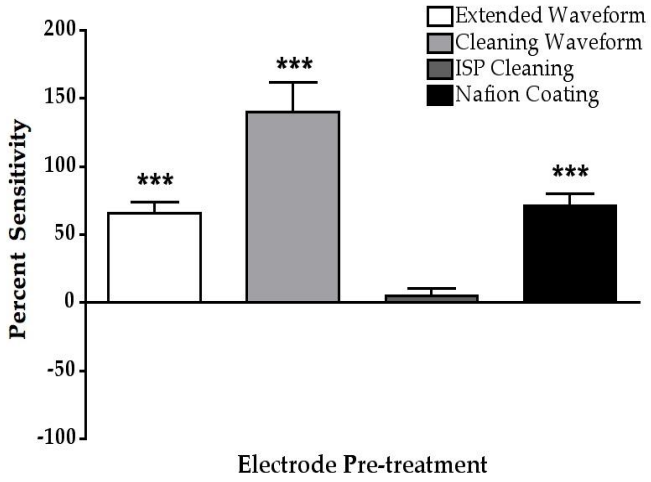

Figure 2.9: The effects of electrode pretreatment on electrode sensitivity. Four different electrode pretreatment methods were compared. Data are shown as percent change in sensitivity of electrodes after treatment compared to before treatment. Except for isopropanol pretreatment, all pretreatment paradigms showed significant increases in electrode sensitivity compared to normalized pretreatment values using one sample *t*-tests. N=5 for extended waveform, n=6 for cleaning waveform, n=5 for isopropanol cleaning, and n=5 for Nafion coating. All values are expressed as means ± standard errors of the mean (SEMs), with differences of $P<0.05$ considered statistically significant. Significant differences are denoted as ***$P<0.001$ compared to pretreatment sensitivity.

waveforms with varying resting or oxidation potentials. Results with the conventional and other waveforms were compared to investigate whether a modified waveform can regenerate the initial electrode response after fouling. Additionally, the effects of various pretreatments of electrodes on fouling were also investigated.

Changes in resting potential and effects on fouling

In this experiment, the effects of various resting potentials on electrode fouling due to serotonin in a chronoamperometric experiment were investigated. For this purpose, electrodes were calibrated prior to and after exposure to 10 μM serotonin for 30 min. Figure 2.10 shows the results of these experiments. Changing the resting potential of the applied waveform does not show significant regeneration of electrode sensitivity after fouling compared to the conventional 0 V resting potential.

Changes in oxidation potential and effects on electrode fouling

Similar to the previous experiment in which resting potentials were altered using chronoamperometry to determine if electrode responses could be regenerated after fouling, additional experiments were carried out to determine if changing the applied oxidation potential leads to regeneration of electrode responses after fouling. In these experiments, the resting potential was held constant at 0.0 V and the oxidative potential was varied between 0.35 V to 0.75 V in 0.10 V increments. Figure 2.11 shows percent changes in electrode sensitivity after fouling compared to before fouling for the various waveforms used. For all values of applied potential, there were no significant differences in loss of electrode sensitivity due to fouling compared to the conventional

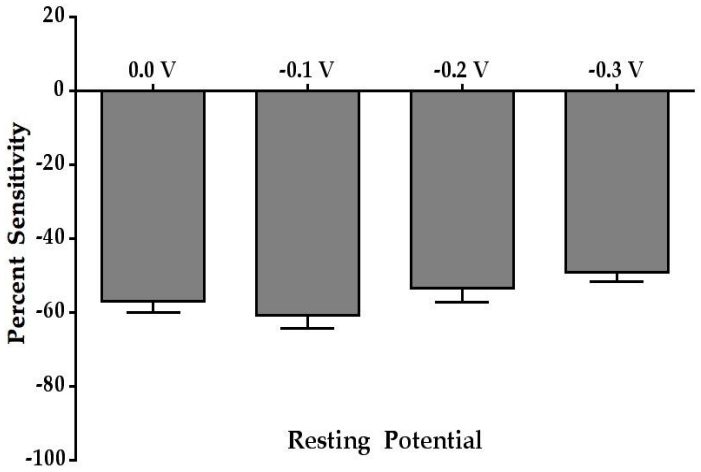

Figure 2.10: Effects of alterations in resting potential on electrode sensitivity after fouling. Percent changes in electrode responses after fouling with high concentrations of serotonin (10 µM) for 30 min using varying resting potentials were determined. Different resting potentials did not result in significant regeneration of electrode sensitivity compared to the convention 0.0 V resting. N=9 for all resting potential values. All values are expressed as means ± standard errors of the mean (SEMs), with differences of $P<0.05$ considered statistically significant.

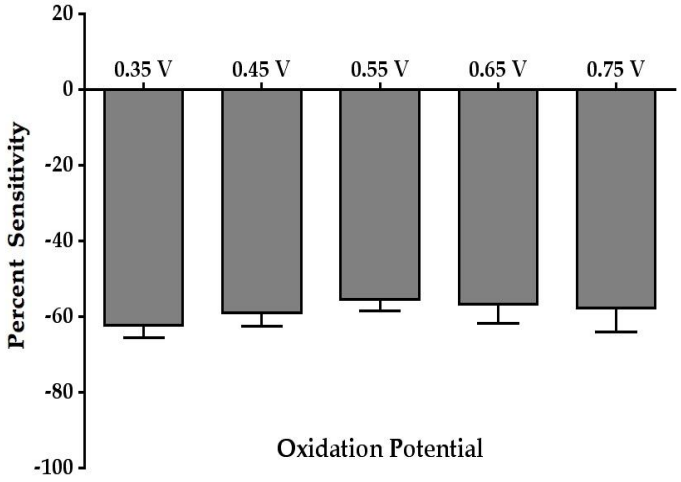

Figure 2.11: Effects of alterations in oxidative potential on electrode sensitivity after fouling. Percent changes in electrode responses after fouling with high concentrations of serotonin (10 μM) for 30 min using varying applied oxidative potentials were analyzed. Different oxidation potentials did not result in significant regeneration of electrode sensitivity compare to the conventional 0.55 V oxidation potential. N=8 for all oxidative potentials. All values are expressed as means ± standard errors of the mean (SEMs), with differences of $P<0.05$ considered statistically significant.

0.55 V applied oxidation potential value. These results suggest that using higher or lower applied oxidation potentials do not lead to regeneration of electrode sensitivity after electrode fouling due to serotonin.

Electrode pretreatments and effects on electrode fouling

The ability of various electrode pretreatments to prevent electrode fouling after exposure to 10 µM of serotonin was investigated. Three different electrode pretreatment protocols were used and compared to fouling of untreated electrodes using the standard chronoamperometry waveform. The electrode pretreatments used were an extended waveform (-0.3 V resting potential and 0.8 V oxidation potential), isopropanol treatment, and a cleaning waveform (procedures previously described). Figure 2.12 shows the percent changes in electrode sensitivity after fouling compared to electrode responses before fouling for control conditions and various pretreatments. Compared to untreated electrodes, treating electrodes with a cleaning waveform before calibration showed a significant regeneration of electrode sensitivity.

2.3.5 Electrode calibration using fast cyclic voltammetry in a flow cell

Unlike calibration of electrodes using chronoamperometry, where serial injections of serotonin or other species are employed, fast cyclic voltammetry calibrations are made using flow-injections of specific concentrations of the species under investigation. During electrode calibration for FCV using 5-µm CFMs, it was necessary to use a flow cell set-up to avoid electrode fouling during calibration. A

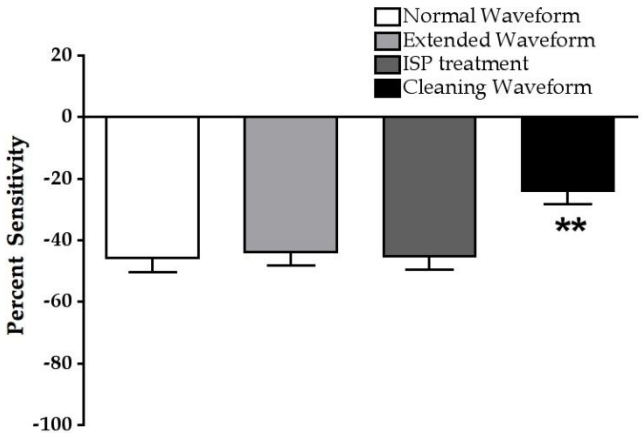

Figure 2.12: Effects of electrode pretreatment on electrode sensitivity after fouling. Here, percent changes in electrode sensitivity after fouling compared to before fouling were determined. For fouling, electrodes were exposed to 10 µM serotonin for 30 min. Untreated electrodes were investigated using the conventional chronoamperometric waveform were used as the control condition. Treating the electrodes with a cleaning waveform with an applied voltage range of +/- 1.8 V at a frequency of 30 Hz for 30 seconds prior to calibration showed significant regeneration of electrode sensitivity compared to control, while the other pretreatments showed no significant changes in electrode fouling. [$F(3,27)=5.363$, $P<0.005$], n=9 for normal waveform, n=7 for extended waveform, n=8 for isopropanol treatment, n = 7 for cleaning waveform. All values are expressed as means ± standard errors of the mean (SEMs), with differences of $P<0.05$ considered statistically significant. Significant differences are denoted as $^{**}P<0.01$ compared to the normal (conventional) waveform.

schematic of the flow cell used in the following experiments is depicted in Figure 2.3. When buffer alone was flowed past the electrode, no change in current was seen. However, when a solution containing an electroactive neurotransmitter was injected into the flow loop, the neurotransmitter flowed past the tip of the electrode and a change in current could be observed. A calibration curve, similar to the one seen in Figure 2.5 for chronoamperometry, could be constructed by injecting several different concentrations of a particular species through the flow cell. A representative calibration curve for fast cyclic voltammetry in a flow cell is shown in Figure 2.13.

2.3.6 Optimizing sensitivity and selectivity by modifying FCV waveforms

To perform fast cyclic voltammetry experiments, it was important to first understand how various waveforms that could be used in fast cyclic voltammetry would affect the sensitivity and selectivity of the electrodes to serotonin, similar to what was done for chronoamperometry. Three waveforms were tested to detect changes in sensitivity to a given concentration of serotonin. The dopamine waveform was used as the control waveform, and the 5-HT waveform at 400 V/s and 1000 V/s scan rates were tested and compared to the dopamine waveform. Figure 2.14 shows percent changes in the oxidation current response compared to dopamine waveform response for 1 μM serotonin. The serotonin waveform at 400 V/s scan rate showed a significant decrease in the electrode response to serotonin, while serotonin waveform at 1000 V/s showed a

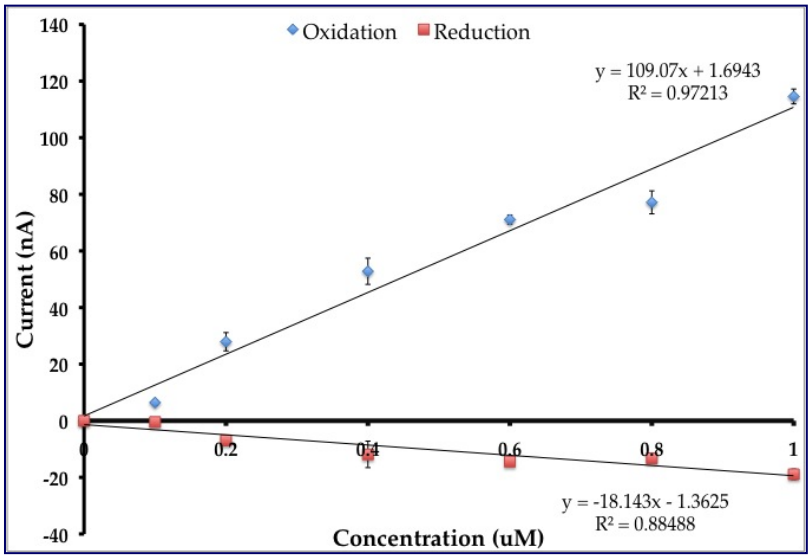

Figure 2.13: Representative serotonin calibration curve using fast cyclic voltammetry in a flow cell. Here, changes in current were measured for injections of different concentrations of serotonin into a flow cell. The serotonin oxidative (blue) and reductive currents (red) showed linear responses to changes in serotonin concentration (0.1-1 µM), r^2=0.9721 and r^2=0.849, respectively.

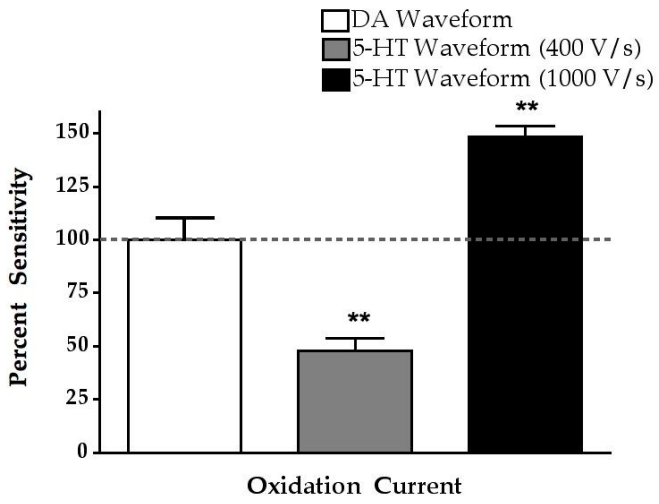

Figure 2.14: Effects of waveform modification and scan rate alterations to increase electrode sensitivity for serotonin. Different waveforms were tested while using fast cyclic voltammetry to sense 1 µM serotonin *in vitro*. The sensitivity for each waveform was compared to the standard DA waveform. The use of the 5-HT waveform at 1000 V/s showed a significant increase in serotonin response, while the 5-HT waveform at 400 V/s showed a significant decrease in serotonin response [$F(2,15)=47$, $P<0.0001$]. N=6 for all waveforms tested. All values are expressed as means ± standard errors of the mean (SEMs), with differences of $P<0.05$ considered statistically significant. Significant differences are denoted in the figures as $^{**}P<0.01$ compared to the dopamine waveform response.

significant increase in the electrode response to serotonin compared to the dopamine waveform.

In addition to monitoring changes in sensitivity to serotonin detected at carbon fiber microelectrodes when different waveforms are applied, we characterized how selectivity for serotonin over other neurotransmitters changes when different waveforms are applied to the working electrodes. This is of particular importance when performing *in vivo* experiments using fast cyclic voltammetry, since many neurotransmitters and electroactive metabolites are present in the brain, often in concentrations much greater than serotonin. For the purpose of detecting serotonin in the brain, it is important that an effective waveform is found that allows the electrode to be more selective for serotonin over other common neurotransmitters.

Figure 2.15 below shows the results from this selectivity experiment. Data were plotted as percent electrode response to 1 µM neurotransmitter vs. 1 µM serotonin for A) dopamine waveform, B) serotonin waveform at 400 V/s scan rate, and C) serotonin waveform at 1000 V/s scan rate. Since the current responses for each neurotransmitter were normalized to the current responses of the electrode to the same concentration of serotonin, the waveform with high selectivity for serotonin should show significantly decreased responses for the other two neurotransmitters. Although the current responses for dopamine and norepinephrine were significant less than that of serotonin in all waveforms used, decreases in responses for these two neurotransmitters were higher when using the serotonin waveform. Using the dopamine waveform, dopamine

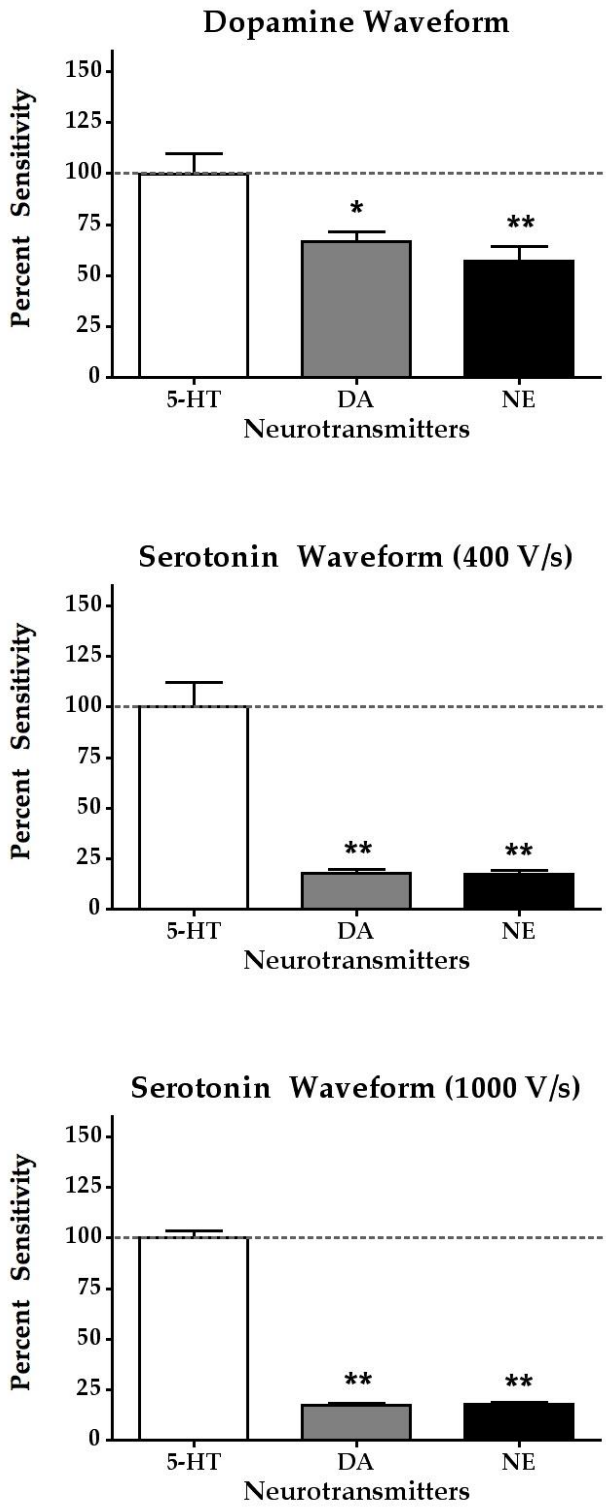

Figure 2.15: Effects of waveform modification and scan rate alterations to increase electrode selectivity for serotonin. Electrode responses to various neurotransmitters (1 μM) were normalized to responses to serotonin. For all three waveforms, serotonin

current responses are significantly greater than those for dopamine and norepinephrine [Dopamine waveform: $F(2,15)=8.7$, $P<0.005$; Serotonin waveform at 400 V/s: $F(2,15)=44$, $P<0.0001$; Serotonin waveform at 1000 V/s: $F(2,15)=460$, $P<0.0001$]. However, using the serotonin waveform, electrode responses for dopamine and norepinephrine are reduced to 20% of the electrode responses for serotonin compared to 70% observed with the dopamine waveform. These results suggest that the serotonin waveform has higher selectivity for serotonin over dopamine and norepinephrine. N=6 for each neurotransmitter tested with each waveform. All values are expressed as means ± standard errors of the mean (SEMs), with differences of $P<0.05$ considered statistically significant. Significant differences are denoted in the figures as $*P<0.05$ and $**P<0.01$, compared to serotonin response for that waveform.

and norepinephrine current values were 70% and 60% of the serotonin current values, respectively but using the serotonin waveform (400 or 1000 V/s scan rate), dopamine and norepinephrine current values drop to less than 20% of the serotonin response. These results suggest that the serotonin waveform is almost five times more selective for serotonin over dopamine or norepinephrine.

2.4 Discussion and conclusions

All of the experiments in this chapter were designed to characterize the responses of carbon fiber electrodes so that their responses to serotonin and other neurotransmitters could be better understood. In addition, we analyzed which waveforms, fabrication techniques, and treatments would allow for maximum sensitivity and selectivity for detecting serotonin so that further experiments could be optimized.

Before testing electrode behavior under varying waveform and/or treatment conditions, it was necessary to understand how carbon fiber microelectrodes respond to various concentrations of neurotransmitters under control conditions. The first set of experiments sought to describe the standard calibration curves of a chronoamperometric experiment that could be created by increasing concentrations of a neurotransmitter (serotonin) serially. Thirty-micron diameter cylindrical carbon fiber electrodes showed linear responses to increasing concentrations of serotonin (200 nM-1 μM) thus validating that the electrode fabrication method was successful. Additionally, these calibration curves showed that using CFMs and chronoamperometry, we can accurately detect concentrations of dopamine and norepinephrine as low as 100 nM

and concentrations of serotonin as low as 200 nM. Ratios of reduction to oxidation currents were calculated from calibration curves created by testing electrode responses to different neurotransmitters. These redox ratios could be used to identify species to a certain extent.

In addition to the importance of high selectivity for serotonin, it is also important that the carbon fiber microelectrodes used in these experiments be sensitive to low levels of serotonin, especially for *in vivo* experiments. The next part of the electrode characterization experiments involved various attempts at maximizing the sensitivity of the carbon fiber microelectrodes to serotonin. This was done in various ways, including altering the resting and applied potentials in chronoamperometry and treating the electrodes with one of four different pre-treatments. It was found that sensitivity was increased the most when the resting potential was set to -0.2 V and the applied potential was 0.7 V. Various electrode pre-treatment methods examined showed that with the exception of cleaning with isopropanol, all other pre-treatments led to increases in electrode response and thus sensitivity to serotonin.

To obtain accurate results throughout an experiment, it is necessary to prevent as much fouling of the electrode as possible. Fouling by adsorption of serotonin and/or proteins in the brain will cause the response characteristics, sensitivity, and selectivity of electrodes to change. This change in electrode responses alters the interpretation of the results of experiments. Therefore, it was important to investigate various anti-fouling or surface regeneration techniques, including altering the resting and applied potentials and using electrode pretreatments. These techniques attempted to maintain as much of

the original sensitivity of the electrodes to serotonin as possible. Alterations in the resting and applied potentials did not significantly prevent fouling. Using an extended waveform or Nafion coating which previously showed beneficial effects on enhancing electrode sensitivity also failed to regenerate electrode sensitivity or prevent electrode surface fouling. By contrast, treating the electrode with a cleaning waveform with an applied voltage range of +/- 1.8 V at a frequency of 30 Hz for 30 seconds prior to calibration showed significant regeneration of electrode sensitivity.

Apart from chronoamperometry, electrode responses to various neurotransmitters were also investigated using fast cyclic voltammetry. Similar to the calibration experiments previously mentioned for chronoamperometry, 5-µm carbon fiber microelectrodes were tested using serial calibration in a flow cell with fast cyclic voltammetry. The smaller electrodes, in this case, also responded linearly to increasing concentrations of serotonin showing high sensitivity and accurate detection of 200 nM of serotonin. Since fast cyclic voltammetry is the technique used for *in vivo* serotonin detection in this laboratory, it was necessary to characterize various waveforms to optimize the sensitivity and selectivity of carbon fiber microelectrodes to serotonin. It was found that the serotonin waveform applied at 1000 V/s scan rate showed the highest current response for serotonin. Additionally, the serotonin waveform at the 400 V/s and 1000 V/s scan rates showed 5 times more selectivity for serotonin over dopamine. Based on these results, the serotonin waveform at 1000 V/s scan rate is best suited for serotonin detection because of its high sensitivity and selectivity for serotonin.

In conclusion, these characterization experiments showed that chronoamperometric results could be improved for detecting serotonin by using -0.3 V as the applied resting potential and 0.7 V as the applied oxidation potential. In addition, treating carbon fiber electrodes with a cleaning waveform (± 1.8 V at 30 Hz for 30 s) prior to experiments showed a significant increase in electrode sensitivity to serotonin. Fouling experiments showed that alterations to the applied resting or oxidation potentials did not prevent loss of sensitivity of the electrodes after fouling. However, using the aforementioned cleaning waveform significantly reduced loss in sensitivity due to fouling. Characterization experiments performed for fast cyclic voltammetry showed that using the serotonin waveform at 1000 V/s significantly increased sensitivity and selectivity for serotonin over dopamine and norepinephrine.

References

1. Dryhurst G (1990) Applications of electrochemistry in studies of the oxidation chemistry of central nervous system indoles. Chemical Reviews 90:795-811.
2. Gerhardt GA, Hoffman AF (2001) Effects of recording media composition on the responses of Nafion-coated carbon fiber microelectrodes measured using high-speed chronoamperometry. J Neurosci Methods 109:13-21.
3. Jackson BP, Dietz SM, Wightman RM (1995) Fast-scan cyclic voltammetry of 5-hydroxytryptamine. Anal Chem 67:1115-1120.
4. Kandel ER, Schwartz JH, Jessell TM (2000) Principles of Neuroscience, 4th Edition. New York: McGraw Hill Professional.
5. Kawagoe KT, Zimmerman JB, Wightman RM (1993) Principles of voltammetry and microelectrode surface states. J Neurosci Methods 48:225-240.
6. Michael DJ, Wightman RM (1999) Electrochemical monitoring of biogenic amine neurotransmission in real time. J Pharm Biomed Anal 19:33-46.
7. Perez XA, Andrews AM (2005) Chronoamperometry to determine differential reductions in uptake in brain synaptosomes from serotonin transporter knockout mice. Anal Chem 77:818-826.
8. Perez XA, Bianco LE, Andrews AM (2006) Filtration disrupts synaptosomes during radiochemical analysis of serotonin uptake: comparison with chronoamperometry in SERT knockout mice. J Neurosci Methods 154:245-255.
9. Wightman RM (1988) Voltammetry with Microscopic Electrodes in New Domains. Science 240:415-420.

10. Wisniewski N, Reichert M (2000) Methods for reducing biosensor membrane biofouling. Colloids Surf B Biointerfaces 18:197-219.
11. Wrona MZ, Dryhurst G (1987) Oxidation chemistry of 5-hydroxytryptamine. 1. Mechanism and products formed at micromolar concentrations. J Org Chem 52:2817-2825.

Chapter 3: Electrode placement determination

3.1 Introduction and background

When performing *in vivo* electrochemistry experiments in mouse brains, it is important to consider the structural and functional effects of implanting a foreign object into the brain. The *in vivo* voltammetery experiments performed in our laboratory use small CFMs (5 or 30 µm in diameter), unlike microdialysis experiments which utilize 200 µm diameter probes (T. E. Robinson and J. B. Justice, 1991). However, it is still important to investigate and to attempt to understand how CFMs implanted into the brain affect brain tissue and physiological functioning, and therefore, our experimental results (J. L. Peters et al., 2004; W. K. Schiffer et al., 2006; D. B. Frumberg et al., 2007; C. M. Mitala et al., 2008). If implanting carbon fiber microelectrodes causes extreme damage and even cell death, normal signaling and/or function of neurons will be inhibited (J. L. Peters et al., 2004). Encapsulation of the electrodes due to inflammatory reactions in the brain might also affect measurements. For all of these reasons, it was important to investigate different methods of observing and monitoring the damage caused by brain probes.

Additionally, one of the primary goals of the research discussed in this chapter was to sufficiently mark the implantation site of the probes to determine whether the electrodes were effectively stimulating and measuring release and reuptake of serotonin in the appropriate brain regions. By attempting to mark the implantation sites of the electrodes, the appropriate stimulation and measurement sites could be confirmed and coordinates for implantation could be honed. Thus, this research was necessary to support *in vivo* experiments planned for the future.

Insertion of various sized probes into the brain causes obvious damage to the neurons in the direct path of the inserted probe (J. L. Peters et al., 2004; W. K. Schiffer et al., 2006; D. B. Frumberg et al., 2007; C. M. Mitala et al., 2008). In the past, studies have been performed characterizing brain tissue damage due to the implantation of microdialysis probes and carbon fiber microelectrode probes. The purpose of these previous studies was to observe the tissue level, metabolic, and behavior deficits that occurred after the implantation of such probes into the mouse or rat brain. These studies revealed that significant local damage in the region of the probe implantation site, whether for microdialysis or carbon fiber microelectrode probes, resulted in significant changes in brain metabolic activity and neuronal signaling (J. L. Peters et al., 2004; W. K. Schiffer et al., 2006; D. B. Frumberg et al., 2007; C. M. Mitala et al., 2008).

In a study performed by Mitala, *et al*., dopamine release was monitored via voltammetry before, during, and after the implantation of a microdialysis probe 220 μm away from the carbon fiber electrode implantation site. It was found that the insertion of the microdialysis probe in the vicinity of the carbon fiber microelectrode caused damage to the surrounding vasculature and also caused changes in the release of dopamine observed at the carbon fiber microelectrode (C. M. Mitala et al., 2008). The release of dopamine as measured by voltammetric methods decreased by 90% after the local implantation of the microdialysis probe, and confirmatory tests proved that this decrease in dopamine release was not due to the dialysate used in the microdialysis procedure but instead was due to disruption of the vasculature in brain regions near the microdialysis and carbon fiber microelectrode implantation sites. These findings imply

that the functioning of other neurotransmitter systems in the brain (such as the serotonergic system) would also be adversely affected by the implantation of brain probes.

Other studies have been performed that focused on metabolic changes in the brain occurring after the implantation of brain probes. In a study performed by Shiffer, *et al.*, it was hypothesized that intracerebral microdialysis transiently altered (decreased) tissue metabolism (W. K. Schiffer et al., 2006). This study monitored the uptake of the glucose analog 18-flurodeoxyglucose (^{18}FDG) by neurons in the brain. As ^{18}FDG enters glucose metabolic pathways, its increased or decreased uptake by neurons in the brain is indicative of the metabolic function of different brain regions. Micro positron emission topography (microPET) was used to monitor the gamma rays emitted indirectly by the positron emitting radionucleotide (in this case Fluoride 18, or F-18). ^{18}FDG injections were made and uptake was measured 1 day prior to the implantation of the microdialysis probe and again at 0.2, 0.5, 1, 2, 5, 7, 15, and 25 days after the implantation of the microdialysis probe (chronic implantation) (W. K. Schiffer et al., 2006). Images obtained using microPET indicated that with time, ^{18}FDG uptake decreases throughout the entire hemisphere ipsilaterial to the implanted probe. In "sham" studies where the microdialysis probe was inserted for only a brief time and then removed, normal metabolism was restored within 5 days after the removal of the microdialysis cannula. The main conclusion to be taken away from this study is that the damage elicited by the implantation of the brain probe (in this case, a microdialysis probe) extends far beyond the local region of the implanted probe (as far as the entire

ipsilateral hemisphere) (W. K. Schiffer et al., 2006). While the implantation of a carbon fiber microelectrode used for voltammetry may not cause metabolic damage that extends quite this far, it is probable that some effect on metabolism of local neurons occurs.

Another study performed by Frumberg, *et al*., sought to determine the behavioral impact of microdialysis probe implantation in rodents (D. B. Frumberg et al., 2007). Frumberg hypothesized that functional metabolic deficits observed following surgical brain injury due to microdialysis probe implantation are associated with changes in cognitive performance in rodents. Novel object recognition tests and general locomotive tests were performed to judge changes in behavior before and after implantation of a microdialysis probe. In the novel object recognition test, cannulated rats showed significant decreases in exploration of the presented novel object when compared to control rats that underwent anesthesia only (D. B. Frumberg et al., 2007). General locomotion tests revealed no significant differences between the cannulated and control groups. This study concluded that significant and persistent cognitive impairment occurs after implantation of a microdialysis probe and that this decrease in cognitive function is consistent with the probe-induced decrease in glucose metabolism in the brain regions surrounding the implanted probe (D. B. Frumberg et al., 2007). Although these studies investigated the effects of a much larger probe than is used in our studies (microdialysis probe has an outer diameter of ~200 µm, while *in vivo* carbon fiber microelectrodes have an outer diameter of ~5 µm), these changes indicate that the disruption of brain tissue can have widespread affects on the function of the brain.

Finally, another study relevant to the work performed in this chapter was reported by Peters, *et al.* in 2004. In this study, Peters and coworkers used carbon fiber microelectrodes with a 7-µm outer diameter in conjunction with voltammetry to monitor tissue-level damage caused by the insertion of these small probes. CFMs were implanted in rat striatum for 4 hours while fast scan cyclic voltammetry was performed. Different methods of marking the extremely small implantation sites were used, including the use of double barreled microelectrodes, electrolytic lesion, and biotinylated dextran amine (BDA) insertion via either iontophoresis or diffusion (J. L. Peters et al., 2004). After implantation, the sites were marked by one of these methods and rats were perfused and horizontal brain sections were prepared and analyzed under the light microscope. One important finding of this study was that light microscopy was insufficient for visualizing tissue damage at the level of the carbon fiber implantation site (J. L. Peters et al., 2004). Therefore, this study made use of electron microscopy to visualize features of the damaged tissue. The findings from the electron micrographs revealed that maximum tissue damage occurred within a 2.5-µm radius around the implantation site, while some damage could be seen in the tissue up to 6.5 µm from the implantation site. Neuronal death only occurred in the direct path of the implanted electrode, but neurons surrounding the electrode implantation site displayed swollen mitochondria and endoplasmic reticulum, depleted numbers of synaptic vesicles, and the development of lysosomes in astrocytes and nerve terminals, all indicating cell distress and neuronal degeneration (J. L. Peters et al., 2004).

The study performed by Peters, *et al*. is of particular importance to the studies presented here, as the primary goal of the present research was to locate the implantation site of the carbon fiber microelectrodes and to study tissue damage around microelectrode implantation sites that can affect voltammetry results. The methods for marking the implantation site were taken from the protocols developed by Peters, *et al.* and include electrolytic lesion and dye marking.

3.2 Materials and methods

3.2.1 *In vivo* surgery and lesions

To prepare mice for *in vivo* experiments, the animals were anesthetized with either ketamine/xylazine or with an isoflurane/oxygen mixture in a knockdown box. The gaseous anesthesia protocol called for an O_2 flow rate of 0.2 to 0.4 psi, with a 4-5% anesthesia mixture when the mouse was in the knockdown box and a 1-2% anesthesia mixture when the mouse was on the stereotaxic frame throughout the surgery and experimentation. Mouse breathing patterns were monitored closely every few minutes throughout the procedure to make certain mice were deeply anesthetized (toe-pinch was used here as well) and not showing signs of respiratory depression. The flow rate of isofluorane was altered based on the aforementioned observations. Injecting physiological saline can also be used to prevent dehydration and increase viability of anesthetized mice.

Mice were checked for appropriate extent of anesthesia using a toe-pinch procedure (no response to toe pinch indicated adequate anesthesia). Eye ointment was

applied to the eyes to protect the cornea from dehydration, and the region of the head to be incised was shaved. Each mouse was place in a stereotaxic frame and the angle of the head was confirmed as flat and firmly fixed in place (the mouse's head should not move when gentle pressure on the skull is applied). The surgical area was first cleaned with water, then with an iodine/alcohol solution, and finally with fresh alcohol wipes (cleaning direction should be from the center to the periphery). An incision was made in the center of the head, and the skin was removed from just behind the eyes to the upper neck using a scalpel or surgical scissors. A few drops of 10% H_2O_2 solution were placed onto the exposed skull to dissolve the pericranial membrane. The 10% H_2O_2 solution was wiped off with a cotton swab approximately 15-30 s after its application, and excess pericranial membrane was removed with scissors.

The position of bregma was measured from the left and right arm of the stereotaxic frame. A mouse brain atlas was used to determine the appropriate distance (in three dimensions) from bregma where holes were drilled and electrodes implanted. A fine-tipped permanent marker was used to mark the point where the drilling occurred. A fine drill bit was used to create a 4 mm (approximate) diameter hole in the skull with the center at the point where the electrode was to be implanted. A reference electrode was inserted into either the neck muscle or the contralateral side of the brain as compared to the working electrode. The working and stimulating electrodes were then inserted into the relevant holes drilled into the skull.

After experiments were complete, mice were sacrificed via cervical dislocation. All of the experimental protocols described here adhered to National Institutes of

Health animal care guidelines and were approved by the Pennsylvania State University Institutional Animal Care and Use Committee. To locate the placement of the electrodes after the experiments were completed, two general techniques were used to mark the implantation sites. First, a dye injection protocol was developed to attempt to mark the implantation site. Next, electrolytic lesions were used to damage the tissue surrounding the implantation site. Brain section staining techniques (Nissl staining and TPH2) were used to visualize brain structures and the implantation sites.

Two different dye injection protocols were developed and used for Evans blue dye staining to mark the placement of the electrodes and the electrode tracts. The first protocol involved injecting a few drops of concentrated Evans blue dye at the top of the electrode tract. The electrode tract was stained due to diffusion of the dye along the tract made by the electrode in the brain. The second protocol involved the fabrication of a pulled glass capillary. The capillary tip was cut, and the capillary was filled with Evans blue dye and was lowered into the brain along the previously made tracts created by the stimulating and working electrodes. Diffusion of the dye from the tip of the capillary into the brain was intended to give information about the electrode placement. The first protocol gave information about the electrode tract, while the second protocol gave information about the final electrode tip placement after histological and immunohistological staining procedures. These stains were not permanent and were thus only good for visual confirmation of the electrode placement during sectioning under the cryostat or microtome.

Electrolytic lesions were created in the brain tissue during *in vivo* experiments by using concentric stimulating electrodes. A 10 V bipolar pulse was applied for 100 seconds in order to "burn" neurons around the stimulating electrode tip, thus creating a lesion in the tissue that could be visualized under the microscope after sectioning with the cryostat or microtome and staining.

3.2.2 Gelatin coated microscope slides

A two-day slide subbing protocol was developed to produce microscope slides that provided the proper adhesive properties for mounting brain sections. On the first day, fresh microscope slides were loaded into metal slide racks. In a 2.25 L Tupperware container, 20 g of Alconox was added to 2 L of hot tap water. The slides in the metal racks were repeatedly dipped into the Alconox solution until soapy, and were then rinsed with cool tap water. Next, an 80% ethanol solution was prepared using a clean 2.25 L Tupperware container by adding 1200 mL of 100% ethanol to 300 mL ddH2O. The slides were then dipped in the ethanol solution and excess ethanol was allowed to drain off. The metal racks were propped up diagonally so that the solution drained to the frosted sides of the slides. Slide racks were covered with aluminum foil and allowed to dry overnight.

On day two, a gelatin coating solution was prepared. A portion of the gelatin solution (3.33%) consisted of a 0.3% chromium potassium sulfate solution. To make 1500 mL of the gelatin solution, 1.5 g of gelatin were added to 1450 mL ddH2O in a large glass beaker. This solution was heated and stirred until the gelatin was completely

dissolved. In a separate beaker, 0.15 g of chromium potassium sulfate was added to 50 mL ddH2O. This solution was stirred until the chromium potassium sulfate was completely dissolved, but was *not* heated. The two solutions were combined in the 2.25 L Tupperware container, and excess surface bubbles were removed. The slides were immersed in the solution for 60 seconds, lifting and lowering the slide racks occasionally. Excess gelatin was drained from the slides, and the slide racks were propped up diagonally so that the solution would drain off to the frosted sides. Again, the slides were covered with aluminum foil and allowed to dry overnight.

3.2.3 Cresyl violet (Nissl) staining

Cresyl violet staining was performed through a series of dehydration, staining, and rehydration steps (G. Paxinos and C. Watson, 1998). It was completed after sectioning the brain using a microtome into various thicknesses (section thicknesses ranged from 10 to 50 µm). The brain sections were then mounted on gelatin-coated microscope slides, described above. The mounted brain sections were allowed adequate time to thoroughly dry to make sure they were properly adhered to the slides. When it was time to begin the Cresyl violet staining procedure, it was necessary to prepare fresh solutions of each of the following before beginning as the timing during the staining protocol was very important: Two xylenes, two 100% ethanol, one 95% ethanol, one 70% ethanol, one distilled water, one 0.5% Cresyl violet solution.

To prepare 500 mL of 0.5% cresyl violet (can be stored in a dark container in the refrigerator and reused several times), 2.5 g of cresylecht violet was mixed with 300 mL

of water, 30 mL of 1.0 M sodium acetate, and 170 mL of 1.0 M acetic acid (G. Paxinos and C. Watson, 1998). The 1.0 M sodium acetate solution was prepared by mixing 13.6 g of granular sodium acetate in 92 mL of water, and 1.0 M acetic acid was made by mixing 29 mL of glacial acetic acid and 471 mL of water. The cresylecht violet, water, sodium acetate, and acetic acid solutions were mixed for at least 7 days on a magnetic stirrer, and then filtered using filter paper.

The slide mounted brain sections were placed into an immunostaining tray filled with xylenes for 5 minutes. After 5 minutes, the slides were then transferred to a fresh immunostaining tray containing xylenes, then 100% ethanol, 100% ethanol, 95% ethanol, 70% ethanol, and distilled water in succession for 5 minutes each. The slides were then transferred to an immunostaining tray containing Cresyl violet staining solution for 30 minutes. After this, the slides were transferred to a tray containing distilled water for 3-5 minutes. Brain sections were then dehydrated by moving them through a succession of solutions for 5 minutes each as follows: 70% ethanol, 95% ethanol, 100% ethanol, and one final 100% ethanol soak. Finally, the slides were submerged in xylenes once more for 5 minutes before using DPX mountant (Sigma) to adhere coverslips to seal the stained sections on the microscope slides.

3.2.4 Tryptophan hydroxylase 2 immunostaining

All incubations and washes for the tryptophan hydroxylase 2 (TPH2) immunostaining protocol were performed on a lab rotator at room temperature, unless otherwise indicated. First, a clean plastic well plate was prepared with mesh well inserts

and the plate was appropriately labeled. The wells were filled to the halfway point with 1x PBS buffer (10x PBS buffer was created by combining 40 g NaCl, 1 g KCl, 1 g KH_2PO_4, and 3.05 g Na_2HPO_4, and then adding ddH_2O to achieve a total volume of 500 mL; pH was adjusted to 7.4). Brain sections (unmounted) were removed from cryoprotectant solution and were placed into the wells containing PBS. The sections were washed 3 times in 1x PBS for at least 5 min each. Next, the sections were incubated in blocking solution (10% goat serum) for 1-2 hours. The 10% goat serum was created by mixing 1 mL of goat serum and 9 mL of 1x PBS buffer.

The sections were then incubated in primary antibody, rabbit anti-TPH2 (Millipore, Billerica, MA), overnight (maximum incubation time of 3 days) at 4°C on a rotator. In order to do this, Eppendorf tubes were labeled for individual tissue sections with antibody information (species raised in, date, dilution). A “no primary” control tube containing only 10% goat serum was included with the incubated tubes. The primary antibody was created by mixing 5 µL of primary antibody with 5 mL of blocking solution (10% goat serum) to create a 1:1000 dilution. Next, 500 µL of the diluted primary antibody were placed into each labeled Eppendorf tube. The brain section(s) were first placed into the “no primary” tube to prevent contamination of antibody from the paintbrush transfer. The remaining brain sections to be stained were transferred into their respective Eppendorf tubes. Finally, the paintbrush used to transfer sections between the well plates and Eppendorf tubes was washed thoroughly.

After incubation in the primary antibody, the sections were removed from the primary antibody tubes and placed into fresh 1x PBS within mesh inserts in clean well plates. These sections were washed three times in 1x PBS for at least 5 min each. The sections were then incubated in secondary antibody, horseradish peroxidase-conjugated goat anti-rabbit (Vector Labs, Burlingame, CA) solution in a glass dish containing 9 wells with 0.9 mL capacity per well for 1-2 hours. To create the secondary antibody solution that was placed into the glass dish, 25 µL of secondary antibody was mixed with 5 mL of blocking solution (10% goat serum) for a 1:200 dilution. After incubation of the secondary antibody in the glass dish, sections were washed 3 times in 1x PBS for at least 5 minutes each.

The sections were then incubated in ABC-peroxidase solution, VECTASTAIN ABC kit (Vector Labs, Burlingame, CA), in a glass dish containing 9 wells of 0.9 mL capacity per well for at least 30 min. It was important to make the ABC-peroxidase solution at least 30 min prior to use (but no more than 1 h before use). To prepare the ABC-peroxidase solution, 5 mL of 1x PBS buffer was measured out. One drop of reagent A and one drop of reagent B were added to this 1x PBS. The solution was then mixed well and was allowed to incubate for the necessary 30 min before applying to tissue sections.

After incubation in the ABC-peroxidase solution, sections were washed 2 times in 1x PBS, and then washed an additional 2 times in 1x TBS (10x TBS was prepared by combining 127 g Tris HCl, 23.6 g Trizma Base, and 87.7 g NaCl before adding enough ddH_20 to create 1 L of solution). The sections were then incubated in diaminobenzadine

(DAB) solution (Sigma Aldrich, St. Louis, MO). First, a 0.1% DAB solution was created by dissolving 1 tablet (10 mg) of DAB in 10 mL ddH_2O for 5-10 min. This mixture was then filtered to remove particulates. The DAB solution was then created by adding 2 mL of the 0.1% DAB mixture to 1 mL ddH_2O, 3 mL of 2x TBS, and 6 µL of H_2O_2. It should be noted that the H_2O_2 should always be added immediately before use, and no sooner. During the incubation of the brain sections in DAB solution, the tubes should be covered with foil to protect the reaction from light. The reaction was monitored as soon as the tissue was exposed to the final DAB solution. The sections were immediately removed from the DAB solution once the sections were sufficiently stained and were placed in ddH_2O to stop the reaction.

Finally, sections were washed 2 times in ddH_2O for at least 5 min each, and the sections were mounted on slides. Sections were allowed to air dry over night.

3.2.5 Chemicals

Ketamine and xylazine was purchased from Henry Schein (Melville, NY). Isofluorane, oxygen, hydrogen peroxide, Evans Blue dye, chromium potassium sulfate, sodium acetate, acetic acid, xylenes, goat serum, and cryoprotectant chemicals were purchased from Sigma Aldrich (St. Louis, MO). Salts used to make the PBS/aCSF buffer were purchased from VWR (West Chester, PA).

3.3 Results

Implantation, sectioning, and staining protocols were carried out and mounted sections were viewed via light microscopy to reveal cellular arrangement and structure.

Figures 3.1 and 3.2 show Nissl stained sections at various magnifications. These stains were used as a proof of concept to show that the staining protocols worked sufficiently after a few minor changes.

In addition to the Nissl staining protocols, tryptophan hydroxylase 2 (TPH2) staining of some of the coronal sections was also carried out. Tryptophan hydroxylase 2 is an enzyme that functions in the synthesis of serotonin in the brain. It catalyzes the reaction that converts L-tryptophan to 5-Hydroxy-L-tryptophan. In staining sections of brain tissue by adding primary and secondary antibodies for TPH2, serotonergic neurons will be stained. Figures 3.3, 3.4, and 3.5 show representative bright-field and dark-field images created using the TPH2 staining protocol. These images were also taken as a proof of concept of the staining procedures.

3.4 Conclusions and future work

The main goal of the work discussed in this chapter was to first find a way to accurately locate carbon fiber microelectrode implantation sites. While many implantation experiments were performed and many methods for marking implantation sites were attempted, no implantation sites could be found using our current methods. Dye protocols involving diffusion of Evans blue into the electrode tract or using a pulled glass capillary gave poor results for electrode marking, as the staining procedures used after sectioning resulted in the dye being washed away. Electrolytic lesions have the potential to be good indicators of where electrodes are implanted into the brain, however, no electrolytic lesions were able to be located anatomically during our studies.

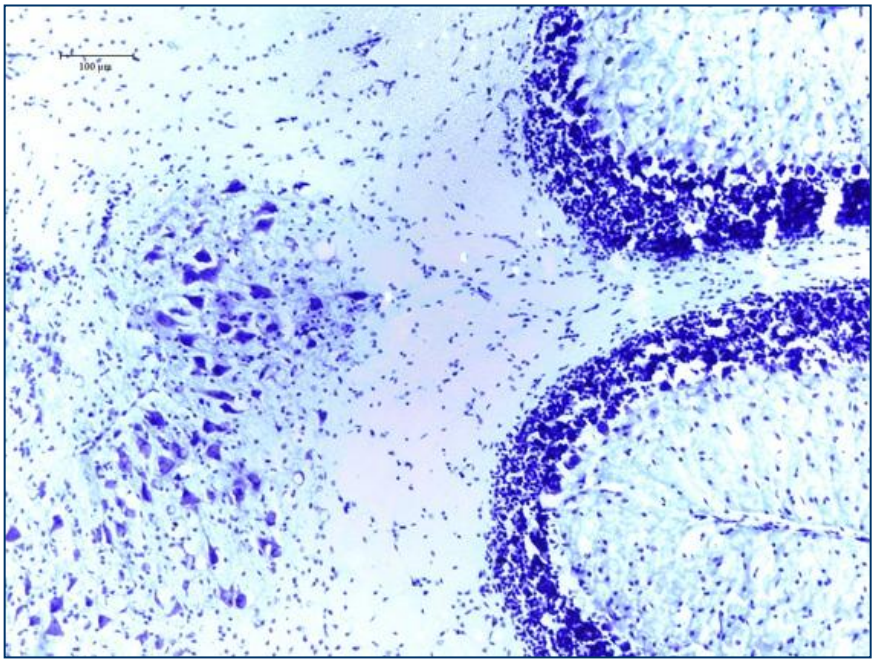

Figure 3.1: Nissl staining of a portion of the mouse cerebellum. This bright field microscopy image was taken as proof of concept that the Nissl staining of the brain sections taken from experiments worked appropriately.

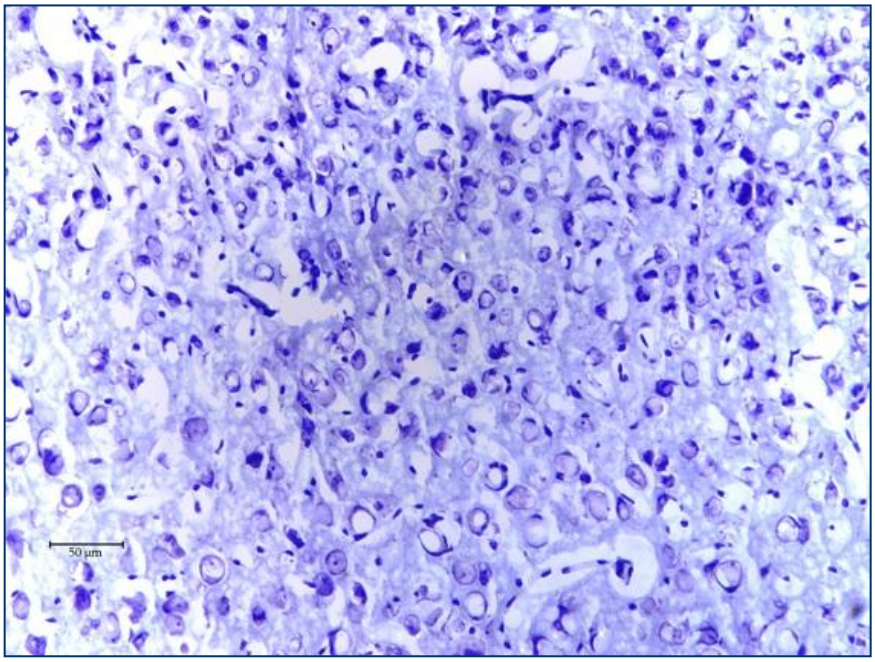

Figure 3.2: Nissl staining of neuronal cell bodies indicating that the Nissl staining protocol was functional. Neuronal cell bodies can be seen with great clarity using the staining protocols specified in these experiments. Damage to areas of the tissue would be easily recognized using this staining method.

Figure 3.3: Bright field microscopy of TPH2 staining of dorsal raphe. The tryptophan hydroxylase 2 immunostaining sufficiently stained serotonin-containing cell bodies in the dorsal raphe of mouse brain.

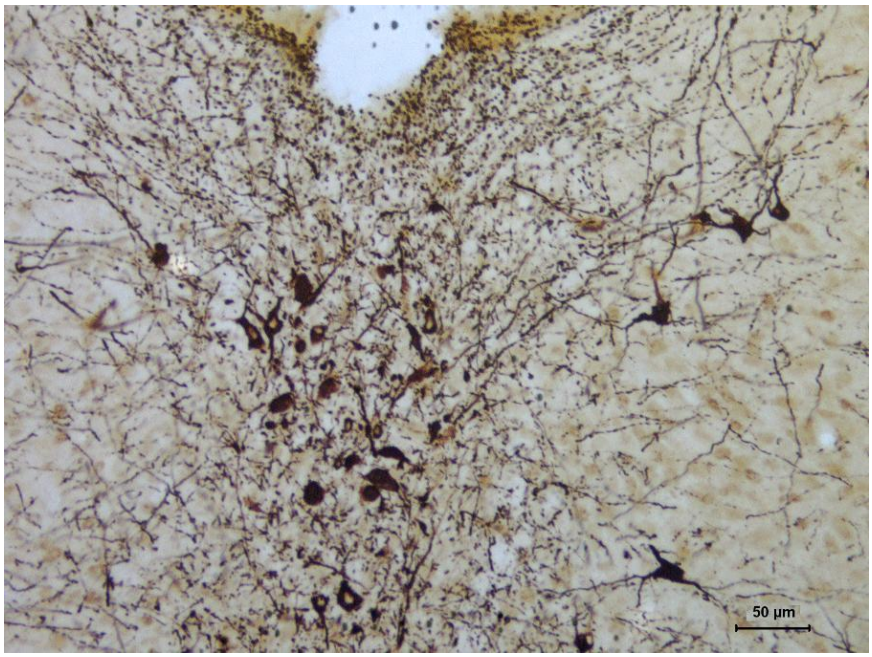

Figure 3.4: Bright field microscopy of TPH2 staining of dorsal raphe. The tryptophan hydroxylase 2 immunostaining sufficiently stained serotonin-containing cell bodies in the dorsal raphe of mouse brain. The cell bodies and dendritic branching patterns of serotonin-containing neurons can be clearly seen at this magnification.

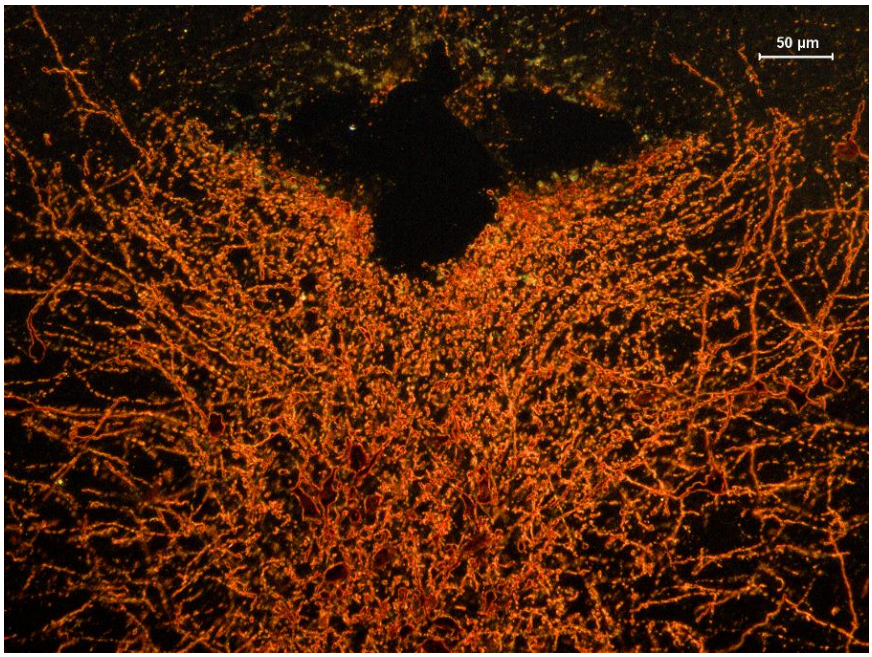

Figure 3.5: Dark field microscopy of TPH2 staining of dorsal raphe. This dark-field image clearly shows the serotonergic neurons (orange fibers) in the dorsal raphe that were stained using the TPH2 staining technique.

It is possible that the implantation sites with the electrolytic lesions or residues of dyes were simply overlooked or missed during our sectioning process. For instance, while the majority of the brain was sectioned using a microtome, only selected sections were mounted onto slides and stained (only a few sections were selected from different regions). The minimum sectioning width used during these experiments was 20 μm, and it is entirely possible that while performing coronal sections, the sections taken and used in the staining protocols did not include sections that contained the electrode implantation sites. In addition, it has been noted that light microscopy might lack sufficient resolution for visualizing electrode implantation sites (J. L. Peters et al., 2004). Therefore, additional experiment will need to be carried to find conditions under which to visualize implantation sites possibly using electron microscopy techniques.

Another method that might be used in future experiments to localize electrode implantation sites would be to section the brain horizontally. This would ensure that each section includes potential damage due to the electrode implantation. Sites where the electrode barrel is just barely seen could then be overlaid with more ventral sections that correspond to depths similar to the length of carbon fiber that extends beyond the pulled glass capillary. Doing so would give a more accurate picture of the depth to which the electrode was implanted into the brain. In conjunction with the staining procedures discussed above and electron microscopy, carbon fiber electrode implantation sites might be more easily located. The ability to locate and to verify implantation sites will eventually allow for the validation of *in vivo* experiments so that we know we are

stimulating and recognizing release and reuptake of serotonin from the correct brain regions.

After electrode implantation sites are able to be easily and consistently located, experiments described in this chapter can be extended to include observations of the changes occurring in the brain due to the implantation of carbon fiber microelectrodes. This might include investigating structural and neuron-level damage due to electrodes and possibly the metabolic and behavioral effects caused by the implantation of these electrodes, similar to what has been done in other investigations on microdialysis probes (W. K. Schiffer et al., 2006; D. B. Frumberg et al., 2007; C. M. Mitala et al., 2008).

References

1. Frumberg DB, Fernando MS, Lee DE, Biegon A, Schiffer WK (2007) Metabolic and behavioral deficits following a routine surgical procedure in rats. Brain Res 1144:209-218.
2. Mitala CM, Wang Y, Borland LM, Jung M, Shand S, Watkins S, Weber SG, Michael AC (2008) Impact of microdialysis probes on vasculature and dopamine in the rat striatum: a combined fluorescence and voltammetric study. J Neurosci Methods 174:177-185.
3. Paxinos G, Watson C (1998) The Rat Brain in Stereotaxic Coordinates, 4th Edition. New York: Academic Press.
4. Peters JL, Miner LH, Michael AC, Sesack SR (2004) Ultrastructure at carbon fiber microelectrode implantation sites after acute voltammetric measurements in the striatum of anesthetized rats. J Neurosci Methods 137:9-23.
5. Robinson TE, Justice JB (1991) Microdialysis in the Neurosciences. New York: Elsevier.
6. Schiffer WK, Mirrione MM, Biegon A, Alexoff DL, Patel V, Dewey SL (2006) Serial microPET measures of the metabolic reaction to a microdialysis probe implant. J Neurosci Methods 155:272-284.

Chapter 4: Investigating coating materials for carbon fiber microelectrodes for in vivo serotonin detection

4.1 Introduction and background information

Within the Andrews laboratory, *in vivo* experiments are currently being performed using fast cyclic voltammetry to measure serotonin release and reuptake rates in the mouse brain. When implanted into the mouse brain, carbon fiber microelectrodes are subject to adsorption of proteins, peptides, and lipids from the brain tissue (S. Alwarappana et al., 2007; C. Rodriguez Emmenegger et al., 2009) and other biochemical and oxidation products of neurotransmitters, including serotonin (B. P. Jackson et al., 1995; B. E. Swamy and B. J. Venton, 2007). Adsorption of these species onto the surfaces of electrodes interferes with the detection of neurotransmitters. The adsorption of proteins and oxidative products to the surfaces of carbon fiber microelectrodes essentially insulates the electrodes and decreases their effectiveness (S. Alwarappana et al., 2007; B. E. Swamy and B. J. Venton, 2007). This fouling process begins to occur in a relatively short time period, which can have profound effects on *in vivo* experiments, as they can sometimes last up to four hours (Y. Singh et al., 2009). For this reason, it is worth considerable time and effort to investigate methods of avoiding fouling, which occurs when carbon fiber microelectrodes are implanted *in vivo.*

While it is necessary to find an electrode coating that will prevent fouling, it is also essential that this coating does not dramatically alter the properties of the electrode so that the *in vivo* measurements are still sensitive and accurate. The coating must not decrease the sensitivity of the electrode to serotonin. In addition, since there

are many neurotransmitters present in the brain in the regions in which electrodes are implanted, it is important that coatings used to prevent fouling do not decrease the selectivity of the electrodes. This will allow the electrodes to continue to record data that allows for the ability to distinguish between serotonin and other common neurotransmitters and their metabolites.

4.2 Materials and methods

To determine what materials might be used to reduce the amount of fouling seen during *in vivo* experiments, it was necessary to create electrodes that had the appropriate amount of sensitivity for serotonin. Blunt cut carbon fiber microelectrodes with a diameter of 30 µm were used to serve this purpose. In addition, common preventative measures that reduce fouling for many types of biological probes were investigated. The results of these investigations were the basis of the electrode coating protocols that will be used in future experiments.

4.2.1 Electrode fabrication

The electrodes used in the following experiments were 30 µm blunt cut carbon fiber microelectrodes. These electrodes were created in a similar manner to the 30 µm cylindrical CFMs, with only slight modifications.

Blunt cut 30 µm disk CFMs

A 30 µm carbon fiber was inserted into a glass capillary using aspiration. The capillaries were then pulled using the capillary puller and the excessively long or curved

portions of the carbon fiber were trimmed. Next, electrodes were cleaned using isopropanol and coated with epoxy for 7 to 8 minutes. The electrodes were then placed in a 100-120 °C oven for 24 to 72 h (no acetone dip). Since the carbon fiber protruding from the glass capillary was completely covered in epoxy, the carbon fiber was cut with a scalpel near the tip of protruding carbon fiber. This created a blunt cut carbon fiber microelectrode, which resulted in only a disk shaped exposed carbon fiber surface while the cylindrical portion of the carbon fiber was completely insulated with epoxy coating.

4.2.2 Fast cyclic voltammetry

Fast cyclic voltammetry experiments were performed using the UEI potentiostat (UNC, Chapel Hill, NC) and the Tar Heel CV program and data were analyzed using FCV custom designed software. For all of the experiments in this section, the dopamine waveform was used with a potential sweep from -0.4 V to 1.2V and back to -0.4 V at 400 V/s scan rate. The calibrations were performed in a flow-injection set-up described in Chapter 2.

4.2.3 Electrode coating protocol

Based on previous work by other groups on various coating materials to increase sensitivity, selectivity, and anti-fouling properties, Nafion, fibronectin, and base-hydrolyzed cellulose acetate were chosen for our investigations (J. Wang and L. D. Hutchins-Kumar, 1986; G. A. Gerhardt and A. F. Hoffman, 2001; S. Marinesco and T. J. Carew, 2002; R. Trouillon et al., 2009). Nafion has been shown to increase electrode

responses to serotonin and thus, increase sensitivity (G. A. Gerhardt and A. F. Hoffman, 2001). Additionally, due to the negative charge imparted at the surface of Nafion-coated electrodes, Nafion can exclude metabolites like ascorbate, 5-HIAA and DOPAC, which are present in high concentrations in brain (G. A. Gerhardt and A. F. Hoffman, 2001). Fibronectin and base-hydrolyzed cellulose acetate have been shown to reduce fouling (S. Marinesco and T. J. Carew, 2002; R. Trouillon et al., 2009). The protocols designed for each coating are described below.

Nafion coating

The Nafion coating protocol described here is adapted from Dr. Gerhardt's research with only slight modifications (G. A. Gerhardt and A. F. Hoffman, 2001). In order to coat CFMs with Nafion, it was necessary to first clean the electrodes by dipping them in isopropanol for 20 seconds and then placing them in an oven for 2 min (oven temperature between 100 and 120°C). Next, electrode tips were briefly dipped into a 5% Nafion solution (tips of electrodes were dipped into the solution for approximately 1 s five times). The electrodes were placed in the oven for additional 5 min. This process was repeated from four to nine times, until the desired selectivity was obtained. For the experiments carried out here, electrodes were coated with Nafion four times. Figure 4.1 shows scanning electron microscopy images of the Nafion coatings on the tips of the blunt cut electrodes at two different magnifications, 1500x and 3500x.

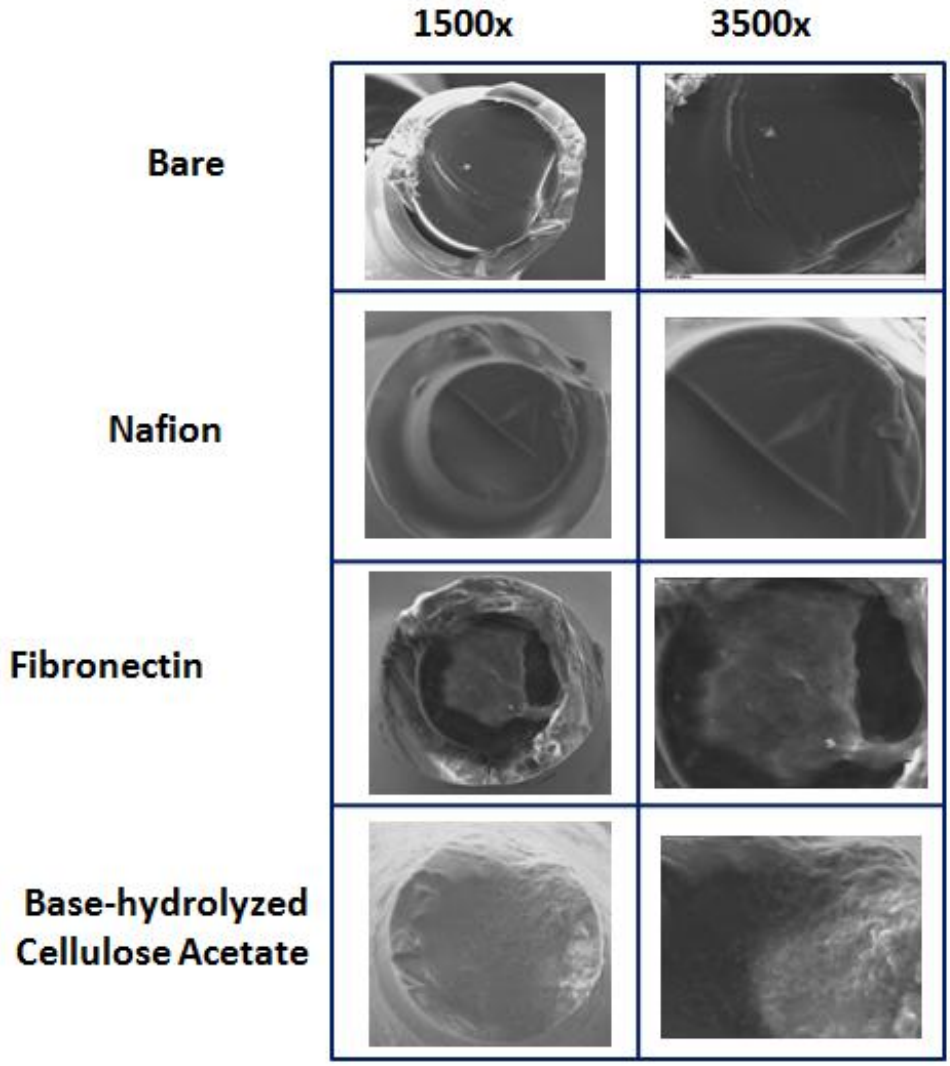

Figure 4.1: Scanning electron microscopy images of electrode tips. These images detail electrode tip surface morphology after coating with Nafion, fibronectin, or base-hydrolyzed cellulose acetate. Bare electrodes showed sharp edges, while Nafion-coated electrodes showed an absence of these sharp edges because of homogenous coating on edge and surface. The fibronectin coating was easily visible as globular growth on the electrode surfaces. Base-hydrolyzed cellulose acetate coating was also easily visible under the scanning electron microscope.

Fibronectin coating

Fibronectin coating is achieved by a dip-coating protocol, similar to the Nafion coating procedure listed above. This protocol was adapted from Trouillon, *et al.* (R. Trouillon et al., 2009). Fibronectin solution (20 µg/ml) was prepared by dissolving 1 mg of fibronectin in 40 mL of Dulbecco's Modified Eagle's Medium (Gibco, Carlsbad, CA). Dissolving the fibronectin in cell media prevented fibronectin denaturation. The fibronectin solution (40 mL) was aliquoted into 40, 1.5 mL Eppendorf tubes. These tubes were then be placed in a -20°C freezer and individual tubes were taken out and thawed before being used to coat electrodes.

To begin the coating procedure, electrodes were placed in isopropanol for 5 min, followed by 10 min of air-drying. Then, electrodes were briefly dipped (for approximately 1 second) in the fibronectin solution and left to air dry for two min. This dipping in fibronectin and drying procedure was repeated six times to create a sufficient coating of fibronectin on the electrode tips. Next, the electrodes were rinsed by dipping them repeatedly into PBS. Finally the electrodes were stored in PBS solution until the time of use.

Base-hydrolyzed cellulose acetate coating

The base-hydrolyzed cellulose acetate coating protocol was adapted from the description of coating protocols from two papers by Wang and Marinesco (J. Wang and L. D. Hutchins-Kumar, 1986; S. Marinesco and T. J. Carew, 2002). The preparation of the base-hydrolyzed cellulose acetate (BCA) coating constituted a more lengthy process.

First, a 1:1 mixture of acetone and cyclohexanone was prepared (7 mL each of acetone and cyclohexanone were mixed in a 20 mL vial). Next, a 5% (5 g/100 mL) cellulose acetate solution was prepared by dissolving cellulose acetate in the 1:1 acetone and cyclohexanone solution. To dissolve the cellulose acetate, the mixture of cellulose acetate in acetone/cyclohexanone solution was stirred for 12 h.

After the 5% cellulose acetate solution was prepared, electrode tips were dipped for approximately 1 s into this solution, separated by 10 min of air-drying at room temperature. This process was repeated 5 times. Cellulose acetate-coated electrodes were hydrolyzed by exposing the electrodes to 0.08 N potassium hydroxide (prepared by adding 62.8 mg KOH to 14 mL of ddH_2O) for 20 minutes. Finally, the electrodes were rinsed using ddH_2O and immersed in 1x PBS/aCSF buffer for at least 10 min and stored in fresh 1X PBS/aCSF solution.

4.2.4 Chemicals

Nafion, fibronectin, cellulose acetate, acetone, cyclohexanone, neurochemicals, and DMEM were purchased from Sigma Aldrich (St. Louis, MO). Salts and isopropanol used to make the PBS/aCSF buffer were purchased from VWR (West Chester, PA).

4.2.5 Data analysis and statistics

Data comparing two means were analyzed using two-tailed unpaired *t*-tests. One-way analysis of variance (ANOVA) was used in cases where more than two means were compared, followed by either Dunnett's Multiple Comparison or Tukey's *post hoc*

tests. All statistical analyses were performed using Graph-Pad Prism v.4 for Mac (GraphPad Software, La Jolla, CA). All values are expressed as means ± standard errors of the mean (SEMs), with differences of $P<0.05$ considered statistically significant. Significant differences are denoted in the figures as $*P<0.05$, $**P<0.01$, and $***P<0.001$.

4.3 Results

There were many considerations involved in determining the best coating to be used to prevent fouling of the carbon fiber microelectrodes. First, an appropriate fouling protocol had to be developed that mimicked the fouling that occurs during *in vivo* studies when electrodes are in contact with the mouse brain. After the fouling protocol was developed, electrodes were coated and tested to observe any changes in sensitivity and selectivity to serotonin that the coatings were associated with. A desirable outcome would be finding a coating that prevents fouling while maintaining or improving electrode sensitivity and selectivity to serotonin. After the changes in sensitivity and selectivity to various neurotransmitters due to the coatings were characterized, the effects of electrode coatings on fouling were determined.

4.3.1 Fouling protocol development

Prior to beginning experiments regarding electrode coatings, we developed a fouling protocol that mimicked the fouling that occurs *in vivo*. Bovine serum albumin (BSA) is a protein that has commonly been used to study protein fouling due to its high adsorption to biosensor surfaces (C. Rodriguez Emmenegger et al., 2009). A solution containing BSA was therefore a viable candidate for use in a fouling protocol and was

tested for its fouling capabilities when electrodes were exposed to BSA solution for 2 hours or overnight. However, the proteins and neurotransmitters found in the brain are far more numerous and the interactions between brain tissue and carbon fiber microelectrodes far more complicated. For this reason, additional experiments were performed to investigate the possibility of using a homogenate of mouse brain tissue to foul the electrodes.

When mice were sacrificed for other experiments, brain tissue was collected and divided into six approximately equal sections. These sections were stored in an -80°C freezer until needed. When fouling experiments were carried out, 0.7 mL of 1x PBS/aCSF buffer was added to an Eppendorf tube containing a thawed sample of brain tissue. A tissue homogenizer was used to create a brain tissue homogenate. Electrodes were then exposed to brain tissue homogenates for either 2 hours or overnight.

Electrodes were calibrated in the flow cell (1x PBS/aCSF buffer used in flow loop) before fouling by measuring the oxidative and reductive current responses to injections of 1 μM dopamine. Serotonin and its oxidized species are highly adsorptive and can cause fouling in and of themselves. Therefore, dopamine was used instead of serotonin to study electrode responses to avoid electrode fouling during electrode calibration. The electrodes then underwent the designated fouling procedures. Some electrodes were submerged in 1x PBS/aCSF buffer overnight as a control. Fouling protocols that were investigated were: 2 hours in BSA, overnight in BSA, 2 hours in homogenized brain solution, and overnight in homogenized brain solution. After fouling, the electrodes underwent a post-fouling calibration to the same concentration of dopamine as in the

pre-fouling calibration. The percent change in oxidative and reductive currents seen in response to dopamine were calculated. In addition, background current, noise, and ΔE (half-wave potential) were monitored pre- and post-fouling to observe the effects of the different fouling protocols on these parameters.

While all fouling methods caused decreases in both oxidative and reductive currents, the method that caused the most significant and consistent decreases in oxidative and reductive currents was exposure to homogenized brain tissue overnight. These results are shown in Figures 4.2 and 4.3. Regardless of fouling method, the background current and noise did not change significantly (Figures 4.4 and 4.5, respectively). Fouling performed in homogenized brain tissue for both the 2 h and overnight durations caused a small, but significant increase in the half-wave potential. When taking all of these results into consideration, homogenized brain tissue was found to be the most effective at fouling electrodes. This fouling method was used in subsequent fouling experiments over other investigated protocols.

4.3.2 Effects of electrode coatings on electrode sensitivity

For an electrode coating that is intended to prevent fouling to be effective, the coating itself must not significantly change the properties of the electrode. The most important feature of an electrode that is implanted *in vivo* is electrode sensitivity or the ability to detect very low concentrations of serotonin. To detect accurately small amounts of serotonin, electrodes implanted into the brain must be extremely sensitive.

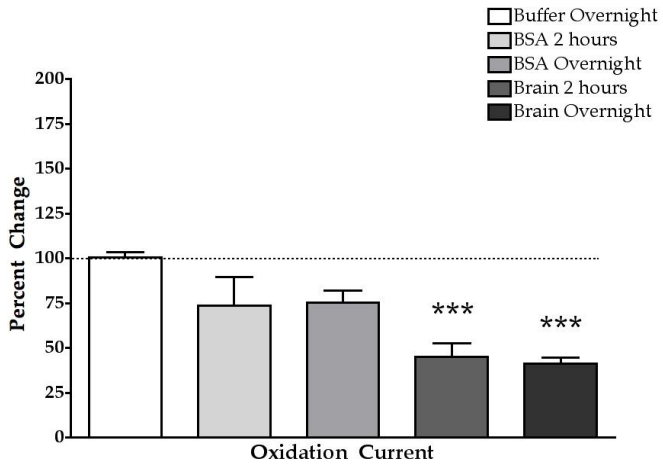

Figure 4.2: Effects of various anti-fouling methods on oxidative current. Data are shown as percent changes in electrode responses (oxidation current) to 1 µM dopamine after fouling as compared to before fouling. Exposure of the electrodes to brain tissue resulted in a significant decrease in oxidation current compared to the control condition (buffer overnight) [$F(4,47)=13$, $P<0.0001$]. Although exposure to bovine serum albumin showed a decrease in current response, it was not significant as compared to control. Exposure to brain overnight showed the most consistent decrease in electrode sensitivity and was chosen as fouling protocol for successive studies. N=11 for buffer overnight, n=8 for BSA 2 hours, n=8 for BSA overnight, n=8 for brain 2 hours, n=17 for brain overnight. All values are expressed as means ± standard errors of the mean (SEMs), with differences of $P<0.05$ considered statistically significant. Significant differences are denoted in the figure ***$P<0.001$ compared to overnight exposure to buffer.

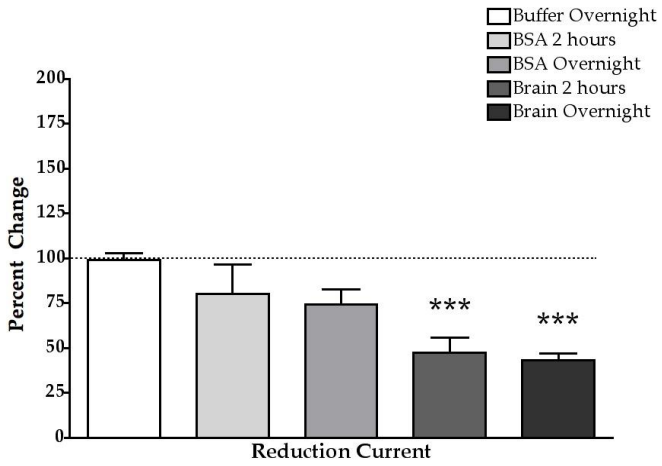

Figure 4.3: Effects of various fouling methods on reductive current. Data are shown as percent changes in electrode responses (reduction current) to 1 µM dopamine after fouling as compared to before fouling. Exposure of electrodes to brain tissue resulted in a significant decrease in reduction current compared to control (buffer overnight) [$F(4,47)=11$, $P<0.0001$]. Although exposure to bovine serum albumin produced a decrease in the current response, it was not significant compare to control. Exposure to brain tissue overnight showed the most consistent decreases in electrode sensitivity and was chosen as fouling protocol for successive studies. N=11 for buffer overnight, n=8 for BSA 2 hours, n=8 for BSA overnight, n=8 for brain 2 hours, n=17 for brain overnight. All values are expressed as means ± standard errors of the mean (SEMs), with differences of $P<0.05$ considered statistically significant. Significant differences are denoted in the figure as ***$P<0.001$ compared to overnight exposure to buffer.

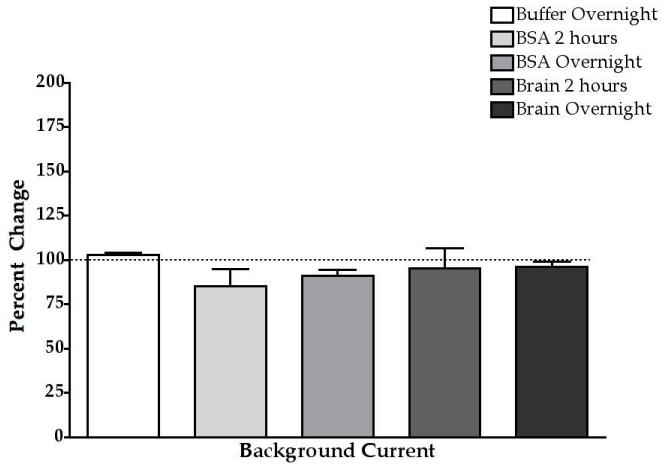

Figure 4.4: Effect of various fouling methods on background current. Data are shown as percent changes in electrode responses (background current) to 1 µM dopamine after fouling as compared to before fouling. Regardless of the fouling method used and time of exposure, the electrodes showed no significant changes in background current response. N=11 for buffer overnight, n=8 for BSA 2 hours, n=8 for BSA overnight, n=8 for brain 2 hours, n=17 for brain overnight. All values are expressed as means ± standard errors of the mean (SEMs), with differences of $P<0.05$ considered statistically significant.

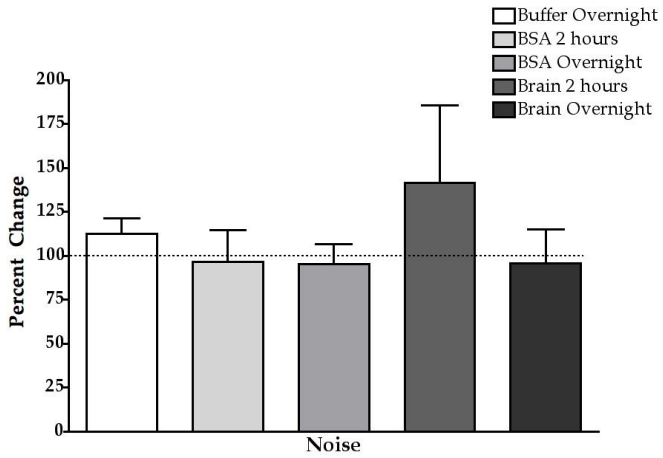

Figure 4.5: Effect of various fouling methods on noise. Data are shown as percent changes in observed electrode noise upon exposure to 1 µM dopamine after fouling as compared to before fouling. Regardless of the fouling method used and time of exposure, the electrodes showed no significant changes in noise. N=11 for buffer overnight, n=8 for BSA 2 hours, n=8 for BSA overnight, n=8 for brain 2 hours, n=17 for brain overnight. All values are expressed as means ± standard errors of the mean (SEMs), with differences of $P<0.05$ considered statistically significant.

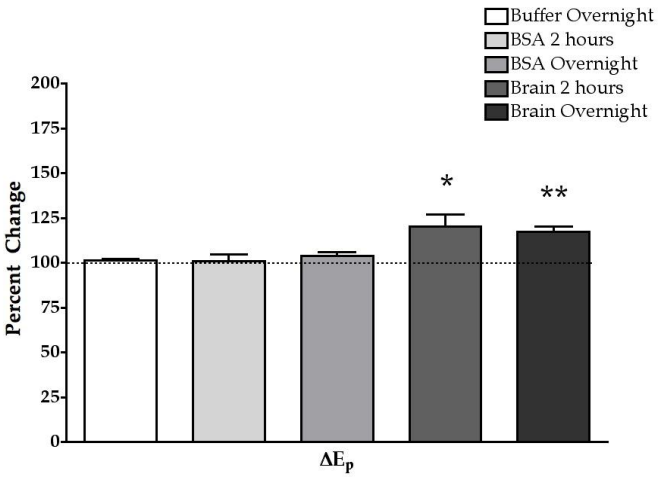

Figure 4.6: Effects of various methods of fouling on peak potential shift. Data are shown as percent changes in electrode responses (half-wave potential) recorded in response to 1 µM dopamine after fouling compared to before fouling. Electrode exposure to fouling protocols showed significant increases in half-wave potential value as compared to control [$F(4,47)=6.3$, $P<0.001$]. N=11 for buffer overnight, n=8 for BSA 2 hours, n=8 for BSA overnight, n=8 for brain 2 hours, n=17 for brain overnight. All values are expressed as means ± standard errors of the mean (SEMs), with differences of $P<0.05$ considered statistically significant. Significant differences are denoted in the figure as $*P<0.05$ and $**P<0.01$ compared to overnight exposure to buffer.

If a coating decreases the sensitivity of a carbon fiber microelectrode, it will prevent the electrode from detecting release and reuptake of serotonin during *in vivo* experiments.

Thus, it was necessary to carry out experiments to investigate how the sensitivity of electrodes changes after they are coated with Nafion, fibronectin, or BCA. Oxidative and reductive current responses to 1 μM dopamine were measured before and after the electrodes were treated with each coating material. The results of these experiments are shown in Figures 4.7 and 4.8.

Electrodes coated with Nafion showed a significant increase in both the oxidative and reductive currents, and thus increased sensitivity. Fibronectin and BCA showed small but not significant decreases in electrode responses (oxidation and reduction currents) due to the applied coating. Thus, if a coating were to be chosen specifically for the purpose of increasing the sensitivity of an electrode, Nafion would be the best choice.

4.3.4 Effects of electrode coating on electrode selectivity

As previously discussed, it is important that electrodes used for *in vivo* experiments be both sensitive to and selective for serotonin. When a probe is implanted into a mouse brain, there are many other neurotransmitters present for which a signal can be detected. Therefore, we tested whether the coatings used on the carbon fiber microelectrodes altered selectivity to a variety of neurotransmitters that are commonly found in the brain. If a coating reduces the ability of an electrode to discern between

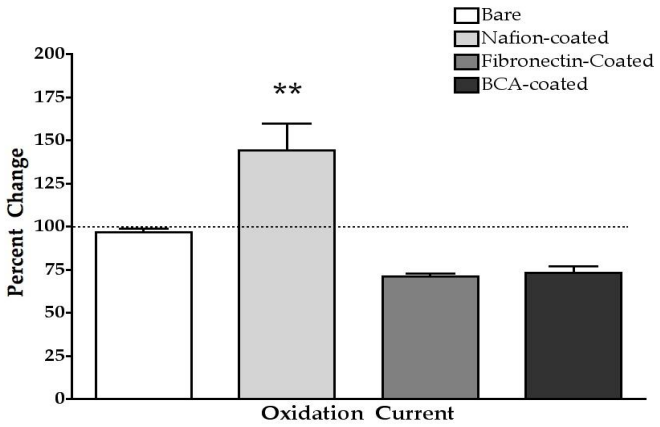

Figure 4.7: Effects of electrode coatings on oxidation currents. Results are shown as percent changes in electrode responses (oxidation current) to 1 µM dopamine after coating compared to before coating response. Only Nafion-coated electrodes showed a significant increase in oxidative current responses due to the coating procedure compared to bare electrodes [$F(3,36)=15$, $P<0.0001$]. N=9 for bare, n=5 for Nafion, n=9 for fibronectin, and n=9 for BCA coated electrodes. All values are expressed as means ± standard errors of the mean (SEMs), with differences of $P<0.05$ considered statistically significant. Significant differences are denoted in the figures as $^{**}P<0.01$ compared to bare electrode responses.

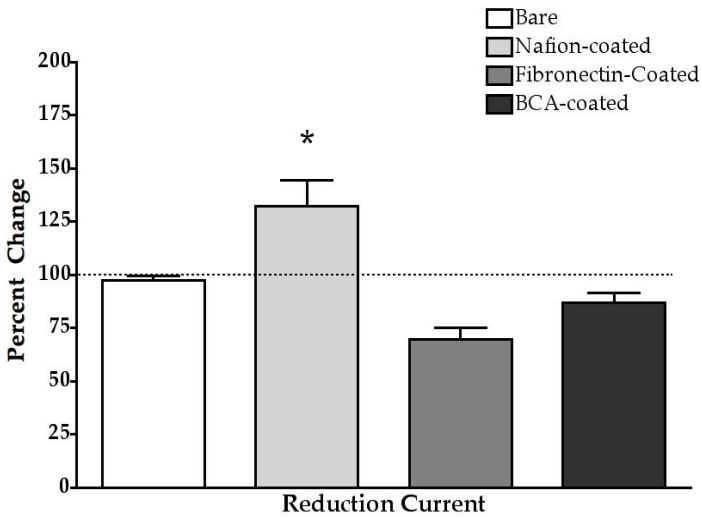

Figure 4.8: Effects of electrode coatings on reductive current. Data are shown as percent changes in electrode responses (reductive current) to 1 µM dopamine after coating as compared to responses before coating. Only Nafion-coated electrodes showed significant increases in reductive current responses due to coating compared to bare electrode [$F(3,38)=12$, $P<0.0001$]. N=9 for bare, n=5 for Nafion, n=9 for fibronectin, and n=9 for BCA coated electrodes. All values are expressed as means ± standard errors of the mean (SEMs), with differences of $P<0.05$ considered statistically significant. Significant differences are denoted in the figures as $*P<0.05$ compared to bare electrode's response.

serotonin and other neurotransmitters, it would not be an effective coating for use in *in vivo* serotonin measurements.

To investigate the effect of the Nafion, fibronectin, and BCA coatings on electrode selectivity to serotonin as compared to bare electrodes, oxidative and reductive current responses to a variety of neurotransmitters were compared. Electrodes were coated with the designated coating or were left bare as the control and were calibrated using a flow-cell set-up. Electrodes were challenged with the following: 1 µM dopamine, 1 µM norepinephrine, 1 µM serotonin, 20 µM 5-hydroxyindoleacetic acid (5-HIAA), 100 µM 3,4-dihydroxyphenylacetic acid (DOPAC), or 100 µM ascorbic acid. Bare- and coated-electrode responses to each of these neurochemicals are shown in Figure 4.9.

Since the electrodes used in *in vivo* experiments are intended to sense serotonin in the mouse brain, it is important that selectivity for serotonin remains relatively high even after being coated with Nafion, fibronectin, or BCA. Therefore, when observing the results from the experiments shown in Figure 4.9, it is necessary to determine which coatings caused significant changes in the oxidative and reductive current responses for different neurotransmitters as compared to bare electrodes. A qualitative summary of the results shown in Figure 4.9 is found in Table 1. The experiments revealed that the BCA-coating caused the smallest differences in oxidative and reductive current responses as compared to bare electrodes. The Nafion-coated electrodes showed a significant decrease in the oxidative and reductive current responses for DOPAC, ascorbate, and 5-HIAA along with a decrease in serotonin current response without

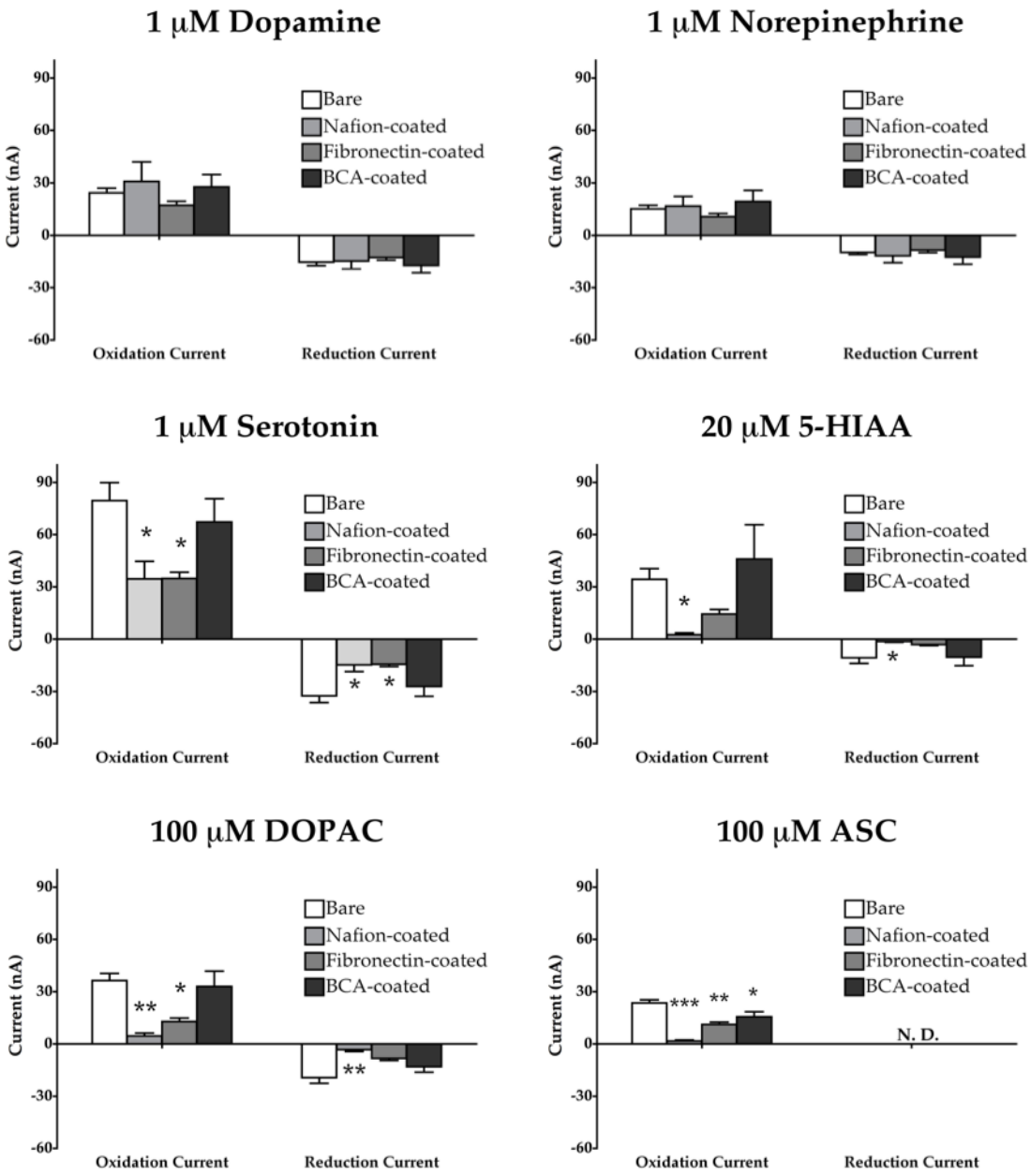

Figure 4.9: Current responses of bare and coated electrodes to different neurotransmitters. The oxidative and reductive current response of bare, Nafion-coated, fibronectin-coated, and BCA-coated electrodes are compared for various neurochemicals. We did not observe significant effects of coating on electrode responses for dopamine and norepinephrine. However, significant differences in electrode responses to various coating are shown for serotonin [oxidative current: $F(3,25)=4.4$, $P<0.05$; reductive current: $F(3,25)=4.7$, $P<0.05$], 5HIAA [oxidative current: $F(3,25)=3.3$, $P<0.05$; reductive current: $F(3,25)=3.6$, $P<0.05$], DOPAC [oxidative current: $F(3,25)=7.7$, $P<0.01$; reductive current $F(3.25)=5.1$, $P<0.01$] and ASC [$F(3.25)=18$,

P<0.0001]. Nafion and fibronectin coatings showed significant decreases in electrode sensitivity for serotonin compared to bare electrode. Only the Nafion coating showed a significant decrease in electrode responses to 20 µM 5-HIAA compared to bare electrodes. Both Nafion and fibronectin showed significant decreases in sensitivity for 100 µM DOPAC compared to bare electrodes. All three coatings including Nafion, fibronectin, and BCA significantly decreased oxidation currents due to 100 µM ascorbic acid compared to bare electrodes. All values are expressed as means ± standard errors of the mean (SEMs), with differences of $P<0.05$ considered statistically significant. N=11 for bare, n=15 for Nafion, n=6 for fibronectin, and n=7 for BCA coated electrodes. Significant differences are denoted in the figures as *$P<0.05$, **$P<0.01$, and ***$P<0.001$ compared to bare electrode responses for that neurotransmitter.

		Percent Change					
		Dopamine	Norepinephrine	Serotonin	5-HIAA	DOPAC	ASC
Oxidation Current	Nafion	↔	↔	↓	↓	↓	↓
	Fibronectin	↔	↔	↓	↔	↓	↓
	BCA	↔	↔	↔	↔	↔	↓
Reduction Current	Nafion	↔	↔	↔	↓	↓	
	Fibronectin	↔	↔	↓	↔	↔	
	BCA	↔	↔	↔	↔	↔	

Table 4.1: Changes in electrode sensitivity for various neurochemicals due to coating. Data are shown as changes in oxidation and reduction currents compared to bare electrodes. Experiments revealed that BCA-coated electrodes showed no significant changes in oxidation and reduction current values for any of the neurochemicals compared to bare electrodes. Nafion and fibronectin coatings showed a decrease in electrode response to serotonin as compared to bare electrodes, thus decreasing electrode selectivity for serotonin over other neurochemicals.

affecting the responses for dopamine or norepinephrine. Thus, Nafion-coating leads to a decrease in selectivity for serotonin over dopamine or norepinephrine as compared to bare electrodes but improves selectivity over acid metabolites. Fibronectin-coated electrodes showed consistent decreases in electrode responses to all of the neurochemicals measured here as compared to bare electrodes. Although this translates into no reductions in selectivity for serotonin over other neurochemicals, the overall decrease in serotonin current suggests that fibronectin is not suitable for highly sensitive serotonin detection. Base-hydrolyzed cellulose acetate-coated electrodes showed no change in electrode responses to any neurochemicals as compared to bare electrodes, thus maintaining the selectivity for serotonin over other neurochemicals.

4.3.5 Effects of electrode coating on electrode fouling

After performing all of the aforementioned experiments that investigated the effects of Nafion, fibronectin, and BCA on electrode sensitivity and selectivity to serotonin and other neurotransmitters, the effects of the electrode coatings on fouling was tested. In order to do this, electrodes were either coated with Nafion, fibronectin, or BCA or were left bare as a control. Pre-fouling oxidative and reductive current measurements were then taken in the flow cell using fast cyclic voltammetry and 1 µM dopamine. After pre-calibration, the electrodes were exposed to homogenized brain tissue overnight (see section 4.3.1). After the electrodes were fouled, post-fouling calibrations were performed using 1 µM dopamine. The percent changes between the

pre- and post-fouling oxidative and reductive current values were calculated and are tabulated in Figures 4.10 and 4.11.

The results of these experiments show that bare- and Nafion-coated electrodes showed significant decreases in both oxidative and reductive currents, indicating that these electrodes were highly fouled. Both the fibronectin- and BCA-coated electrodes showed reduced sensitivity to electrode fouling as compared to bare electrodes.

4.4 Discussion and conclusions

The experiments discussed in this chapter were performed to find a suitable coating for carbon fiber microelectrodes that would reduce the fouling that occurs while the electrode is implanted into the mouse brain. Different fouling materials and exposure times were investigated to mimic the high level of fouling observed in *in vivo* experiments. Exposure to homogenized brain tissue overnight was determined to mimic the fouling that occurs during *in vivo* experiments since the fouling material (homogenized brain tissue) is similar to the environment that the electrodes are exposed to during *in vivo* measurements. Fouling in homogenized brain tissue resulted in high and more consistent electrode fouling.

The effects of the coatings on electrode sensitivity and responses to 1 µM dopamine were measured and compared to bare electrode responses. Only the Nafion coating showed a significant increase in electrode sensitivity, while the other two coatings showed no significant differences in electrode responses as compared to bare electrodes. All of the coatings tested showed no significant differences in other

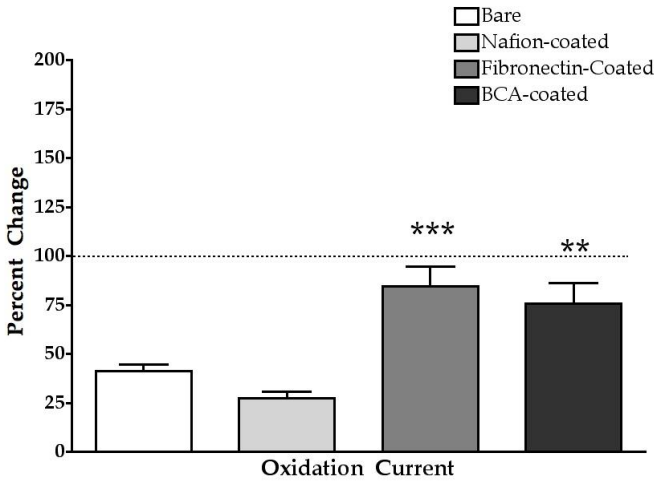

Figure 4.10: Effects of electrode coatings on oxidation current after fouling. Data are shown as percent changes in electrode responses (oxidative current) to 1 µM dopamine after fouling compared to before fouling response. Fibronectin- and BCA-coated electrodes showed significantly higher oxidation current responses after fouling compare to bare electrodes [$F(3,43)=18$, $P<0.0001$]. These results suggest that fibronectin and BCA are fouling resistant coatings while Nafion is not fouling resistant. N=18 for bare, n=15 for Nafion, n=9 for fibronectin, n=9 for BCA coated electrodes. All values are expressed as means ± standard errors of the mean (SEMs), with differences of $P<0.05$ considered statistically significant. Significant differences are denoted with $^{**}P<0.01$ and $^{***}P<0.001$ compared to bare electrode responses after fouling.

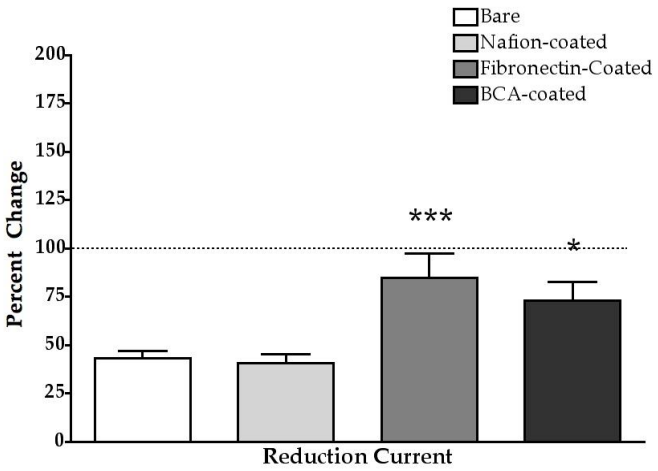

Figure 4.11: Effects of electrode coatings on reduction current after fouling. Data are shown as percent changes in electrode responses (reductive current) to 1 µM dopamine after fouling compared to before fouling response. Fibronectin- and BCA-coated electrodes showed significantly higher reduction current responses after fouling compared to bare electrodes [$F(3,43)=10$, $P<0.0001$]. These results suggest that the fibronectin and BCA coatings are fouling resistant, while the Nafion coating is not fouling resistant. N=18 for bare, n=15 for Nafion, n=9 for fibronectin, n=9 for BCA coated electrodes. All values are expressed as means ± standard errors of the mean (SEMs), with differences of $P<0.05$ considered statistically significant. Significant differences are denoted in the figures as $*P<0.05$ and $***P<0.001$ compared to bare electrode responses after fouling.

electrode properties including background current, noise, or half-wave potential. These results suggest all three coatings are viable options for dopamine measurements.

Electrode responses to these coatings were further tested to investigate selectivity to detect serotonin over other neurochemicals. Due to the high adsorption of serotonin on the surfaces of carbon fiber microelectrodes, a much higher current response is seen as compared to dopamine and norepinephrine. Therefore, bare electrodes have high selectivity for serotonin over dopamine, norepinephrine, and other neurochemicals. Investigations of electrode responses to various neurochemicals for each coating revealed that fibronectin showed a decrease in electrode response to all neurochemicals investigated, while the BCA-coating showed no significant shift in electrode responses compared to bare electrodes. The Nafion coating showed a varied response, where no significant change in electrode responses to dopamine or norepinephrine were observed, but a significant decrease in the responses to other neurochemicals including serotonin was seen.

Experiments to study the anti-fouling properties of these coating materials showed interesting results. These studies revealed that both fibronectin and BCA coatings were the most effective at preventing fouling, while Nafion showed no significant change in electrode fouling compared to bare electrodes.

From this information, a tentative conclusion can be drawn as to which electrode coating is most useful in preventing electrode fouling for the detection of serotonin *in vivo*. While Nafion increased the sensitivity of electrodes to dopamine, it did not prevent

fouling and decreased electrode selectivity of serotonin over dopamine or norepinephrine, thus making it unsuitable for *in vivo* serotonin detection. Fibronectin, however, caused a significant decrease in fouling as compared to bare electrodes but showed a significant decrease in electrode responses to all of the neurochemicals including serotonin, thus making it unsuitable for serotonin detection. On the other hand, the BCA coating showed fouling resistance without interfering with electrode sensitivity or selectivity (compared to bare electrodes) making it the best suited material among these three for *in vivo* serotonin detection.

Although the BCA coating was found to be fouling resistant while maintaining selectivity and sensitivity similar to bare electrodes, it is not an ideal coating. Low concentrations of serotonin in the brain along with very high concentrations of other electroactive neurochemicals necessitate enhancement in electrode sensitivity and selectivity in order to achieve accurate and precise *in vivo* serotonin measurements. For this reason, investigations will be continued within the Andrews laboratory and will test a broader spectrum of coatings, including chitosan, carbon nanotubes, and polypyrrole.

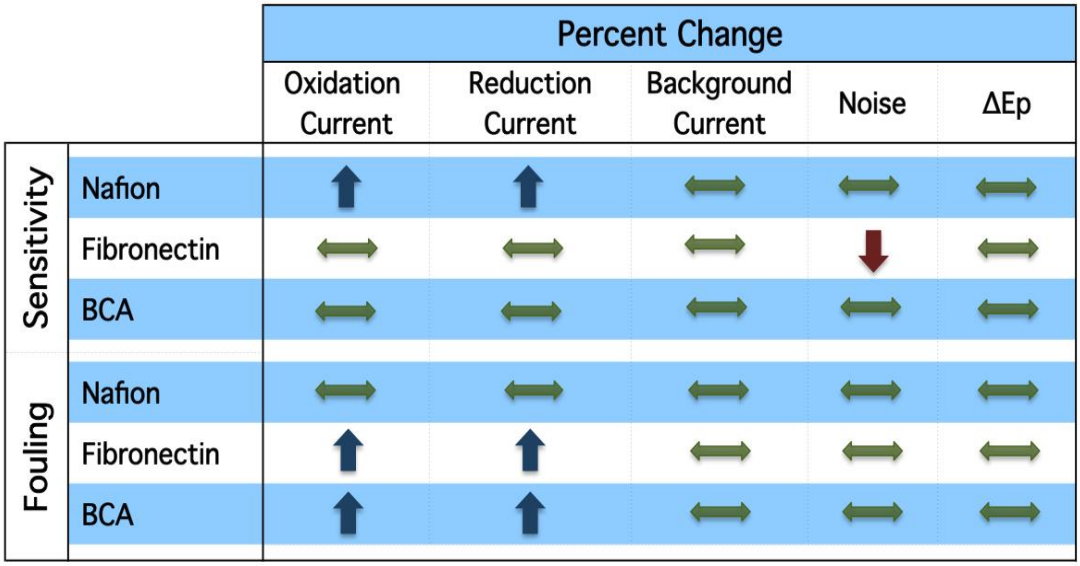

Table 4.2: Change in electrode characteristic responses to 1 µM dopamine for various coatings and fouling. Data are summarized as changes in various electrode characteristics after coating and after fouling compared to bare electrodes. Oxidation and reduction current responses were significantly increased after Nafion-coating, while noise was significantly decreased after fibronectin-coating. Fibronectin- and BCA-coatings showed increased oxidation and reduction currents compared to bare electrodes after fouling, suggesting fouling resistant properties of these two coatings.

References

1. Alwarappana S, Butcherb KS, Wonga DK (2007) Evaluation of hydrogenated physically small carbon electrodes in resisting fouling during voltammetric detection of dopamine. Sensors and Actuators B: Chemical 128:299-305.
2. Gerhardt GA, Hoffman AF (2001) Effects of recording media composition on the responses of Nafion-coated carbon fiber microelectrodes measured using high-speed chronoamperometry. J Neurosci Methods 109:13-21.
3. Jackson BP, Dietz SM, Wightman RM (1995) Fast-scan cyclic voltammetry of 5-hydroxytryptamine. Anal Chem 67:1115-1120.
4. Marinesco S, Carew TJ (2002) Improved electrochemical detection of biogenic amines in Aplysia using base-hydrolyzed cellulose-coated carbon fiber microelectrodes. J Neurosci Methods 117:87-97.
5. Rodriguez Emmenegger C, Brynda E, Riedel T, Sedlakova Z, Houska M, Alles AB (2009) Interaction of blood plasma with antifouling surfaces. Langmuir 25:6328-6333.
6. Singh Y, Sawarynski LE, Michael HM, Ferrell RE, Murphey-Corb MA, Swain GM, Andrews AM (2009) Boron-Doped Diamond Microelectrodes Reveal Reduced Serotonin Uptake Rates in Lymphocytes from Adult Rhesus Monkeys Carrying the Short Allele of the *5-HTTLPR*. ACS Chemical Neuroscience
7. Swamy BE, Venton BJ (2007) Carbon nanotube-modified microelectrodes for simultaneous detection of dopamine and serotonin in vivo. Analyst 132:876-884.

8. Trouillon R, Cheung C, Patel BA, O'Hare D (2009) Comparative study of poly(styrene-sulfonate)/poly(L-lysine) and fibronectin as biofouling-preventing layers in dissolved oxygen electrochemical measurements. Analyst 134:784-793.
9. Wang J, Hutchins-Kumar LD (1986) Cellulose acetate coated mercury film electrodes for anodic stripping voltammetry. Anal Chem 58:402-407.

Chapter 5: Summary

The purpose of the experiments discussed within this thesis was to modify and improve carbon fiber microelectrodes used in conjunction with various voltammetric methods to monitor serotonin *in vivo* and *ex vivo*. Being able to accurately detect release and reuptake of serotonin in the mouse brain will help advance the overall goal of the Andrews' laboratory in understanding the role of serotonin in the etiology of depression and anxiety disorders. Thus, improving electrodes for use in techniques such as chronoamperometry and fast cyclic voltammetry is an important first step in furthering the understanding of the serotonergic neurotransmitter system.

Electrode characterization experiments were performed to better understand various methods of improving the sensitivity and selectivity of carbon fiber microelectrodes. Investigations were performed to understand how altering the applied voltage waveform in chronoamperometry experiments could improve electrode sensitivity and selectivity to serotonin. In addition, experiments were performed to find effective electrode pretreatments, such as a cleaning waveform, to increase sensitivity to serotonin. This cleaning waveform was also shown to be effective in preventing sensitivity loss after electrode fouling. Since fast cyclic voltammetry is used in *in vivo* experiments, it was also necessary to investigate methods of improving sensitivity and selectivity in the 5-µm carbon fiber microelectrodes as well. Using the serotonin waveform at 1000 V/s showed significant increases in both sensitivity and selectivity to serotonin.

In future experiments performed within the Andrews' lab, it would thus be beneficial to use the waveforms and techniques that were shown to improve electrode sensitivity and selectivity to serotonin. Further investigations could be performed to continue to try to improve sensitivity and selectivity of the electrodes and to find more methods for preventing sensitivity loss after fouling.

In vivo voltammetry experiments performed in the Andrews' lab attempt to monitor serotonin release and reuptake in the frontal cortex of mouse brains. After obtaining results from these voltammetry experiments, it is important to confirm that the stimulating and working electrodes were placed into the correct brain regions (the dorsal raphe and frontal cortex, respectively). In order to do so, various dye and lesion techniques were tested. These experiments were preliminary and no conclusive results were obtained, although Cresyl violet and TPH2 staining techniques were found to be effective methods for visualizing brain anatomy. Further work must be performed with this project in order to find a successful and consistent method of marking electrode implantation sites.

Coating experiments were performed on 5 µm carbon fiber microelectrodes to investigate preventative capabilities of various coatings against fouling. In addition, it was necessary to find a coating that did not reduce the sensitivity or selectivity of electrodes to serotonin. Of the coatings tested thus far, it was found that base-hydrolyzed cellulose acetate was most effective at preventing fouling without reducing the ability of the electrode to detect serotonin. While this experiment showed favorable

results for BCA, further experiments should be performed to search for coatings that will further improve electrode function and reduce fouling. Some suggested coatings to continue to research are chitosan, carbon nanotubes, and polypyrrole. Combinations of different coatings may also be attempted as well.

Creating a carbon fiber microelectrode that can detect and monitor serotonin *in vivo* and *ex vivo* with high sensitivity and selectivity is a complicated problem. Many challenges arise when trying to develop an electrode that is sensitive to small amounts of serotonin, can detect and recognize serotonin even in the presence of many other neurotransmitters, and is resistant to fouling. This thesis began to investigate multiple methods which could help improve carbon fiber microelectrode performance for use *in vivo* and *ex vivo*, yet much work can still be done to further develop more effective electrodes for the purposes of the Andrews' laboratory.

ACADEMIC VITAE

LAUREN SAWARYNSKI

256 Atherton Hall
University Park, PA 16802
Cell: (814) 880-0729

les5086@psu.edu

200 Brothers Ct
Port Matilda, PA 16870
Home: (814) 861-2044

ACADEMIC PROFILE

Fourth year Bachelor of Science candidate in Bioengineering with a Materials Science and Engineering option.

EDUCATION

The Pennsylvania State University — **University Park, PA**
The Schreyer Honors College — Graduating on May 14, 2010

RELEVANT COURSES

Calculus with Analytic Geometry I & II
Experimental Chemistry (Labs) I & II
Physics Mechanics
Nutrition
Human Physiology with Lab
Wave Motion and Quantum Physics
Vector Calculus
Organic Chemistry I
Bio-continuum Mechanics
Biothermodynamics
Honors Introduction to Psychology
Biomedical Instrumentation Lab
Material Science of Polymers
Effective Speech
Biology: Basic Concepts and Biodiversity
Bioengineering: Clinical Correlations
Tissue Engineering
Biomedical Surfaces
Chemical Principles I & II (Honors)
Honors Rhetoric and Composition
Computer Science (MATLAB based)
Honors Differential Equations
Physics Electricity and Magnetism
Neuroanatomy, Behavior, and Health
Honors Cell and Molecular Bioengineering
Analysis of Physiological Systems
Physiological Simulation Laboratory
Introduction to Materials Science
Honors Bioengineering Research and Design
Biomedical Instrumentation and Measurements
Data Analysis & Experimental Design (Statistics)
Microbiology with Lab
Materials Characterization
Biomedical Materials
Human Anatomy with Lab

HEALTH CARE EXPERIENCE

Volunteer at Mount Nittany Medical Center — **State College, PA**
August 2008-present

-Work in the Emergency Department to assist doctors and nurses in keeping patients and their families calm and comfortable
-Help nurses by restocking medical equipment and materials to help the department run smoothly
-Currently have over 180 hours of experience, with a goal of 500 hours to be completed by graduation in May 2010

RESEARCH EXPERIENCE

Prof. Anne Andrew's Neuroscience Laboratory — **University Park, PA**
Undergraduate Research Assistant
August 2007 - present

-Currently developing hands-on chemical and biological laboratory experience in the exploration of the function of serotonin in the brain
-Developing and carrying out experiments to enhance sensitivity and selectivity of microelectrodes used in electroanalytical techniques for detection of serotonin release and reuptake *in vitro* and *in vivo*

POSTERS AND PUBLICATIONS

Boron-doped diamond microelectrodes reveal reduced serotonin uptake rates in lymphocytes from adult rhesus monkeys carrying the short allele of the 5-HTTLPR — **ACS Chemical Neuroscience**, Published 2009
Singh YS, Sawarynski LE, Michael HM, Ferrell RE, Murphey-Corb MA, Swain GM, Patel BA, Andrews AM.

Investigation of materials to reduce fouling of carbon fiber microelectrodes for the detection of serotonin *in vivo* — **Society for Neuroscience**, Poster, 2009
Sawarynski LE, Singh YS, Patel BA, Andrews AM.

WORK EXPERIENCE

Ortho-Clinical Diagnostics, Johnson & Johnson — **Raritan, NJ**
Intern — May-August 2007
-Learned to use constructive criticism from peers and superiors to improve the quality of my work
-Gained flexibility and time management by helping with many different projects simultaneously
-Increased interpersonal communication skills by working with employees at varying levels of expertise

LEADERSHIP AND ACTIVITIES

Engineering Ambassador — **University Park, PA**, May 2009-present
-Travel to high schools around Pennsylvania to give presentations about Bioengineering and to encourage students to become active in science and math

Make the Machine Engineering Camp Counselor — **University Park, PA**, July 2008
-Acted as a mentor for high school girls interested in entering the field of engineering
-Helped organize and lead activities to pique girls' interest in engineering

Women in Engineering Program Orientation (WEPO) — **University Park, PA**, August 2007-present
-Acted as a mentor to groups of 6 incoming freshman women in engineering majors each year
-Led and communicated with my group of freshman women throughout each year, providing both academic and non-academic advice to help make their transition to college occur smoothly

Women in Engineering Program (WEP) — **University Park, PA**, 2006-present
-Active member of the Women in Engineering Program

Girl Scout Saturdays — **University Park, PA**, 2006-2009
-Volunteered as a mentor to young Girl Scouts ranging in age from kindergarten to juniors in high school.
-Helped teach girls about math and science in a fun and interactive learning environment

AWARDS AND RECOGNITION

American Reinvestment and Recovery Act National Institute of Mental Health Summer Research Award — **2009**

Phi Kappa Phi — **March 2009**
-Member of the national honors society, which recognizes academic excellence in all disciplines

Tau Beta Pi — **December 2008**
-Member of the national engineering honors society